2011

Performance characterization of a pilot-scale oxygen enriched-air and steam blown gasification and combustion system

Cuong Van Huynh
Iowa State University

Performance characterization of a pilot-scale oxygen enriched-air and steam blown gasification and combustion system

By

Cuong Van Huynh

A thesis submitted to the Graduate Faculty in partial fulfillment of the requirements for the degree of:

MASTER OF SCIENCE

Major: Mechanical Engineering

Program of Study Committee:

Song-Charng Kong, Major Professor

Theodore Heindel

D. Raj Raman

Iowa State University

Ames, IA

2011

Table of Contents

List of Figures

List of Tables

Acknowledgement

First of all, I would like to thank my major professor Dr. Song-Charng Kong for offering me the opportunity to work on a project that has great potential to contribute to solving the world problems of energy crisis and increasing greenhouse gas emissions. Throughout the project, Dr. Kong has fully committed himself to help me when confusions or difficulties arose. Additionally, Dr. Kong provided me with many professional insights and guided me toward successful conclusions.

I would also like to express my gratitude to Dr. Theodore Heindel and Dr. D. Raj Raman for spending their valuable time to serve as my committee members. Dr. Heindel and Dr. Raman have provided excellent feedback for improvement of this thesis.

I owe much to Patrick Johnston and Frontline Bioenergy for their engineering support. They have given me much advice on analytical equipment operations and effective data collection methods. Moreover, I valued their friendships and the opportunity to share in their expertise and knowledge in the area of biomass gasification.

Finally, I would like to thank my family members and research group members for their support. They have always encouraged me to do my best work and have served as my source of inspiration.

Abstract

The use of air as biomass gasifying agent yields low heating value product gas and is only suitable for heat and power applications. Steam and oxygen gasification on the other hand can increase gas heating value as well as main gas constituents suitable for production of liquid fuels through synthesis processes.

Experiments were carried out to investigate the influence of using oxygen enriched-air and steam mixture as gasifying agents on syngas composition, heating value, fuel-N conversion to ammonia, and NO_X emissions during gasification and combustion. The oxygen content in the enriched air was varied from 21% (v/v, atmospheric air) to 45% and 80% on dry basis. On wet basis, the oxygen percentages are equivalent to 30% and 40%. All tests were maintained at fixed bed temperature of 800 °C and steam to biomass ratio (S/B) approximately 0.17. In addition tests were also conducted using three different biomass feedstocks with nitrogen content varying from 0.05 to 1.4 wt%. The NO_X emissions from syngas combustion were characterized from different burner operating conditions such as varying heat rates and equivalence ratio.

It was shown that oxygen-enriched air and steam gasification favors the increase of combustible gas components such as H_2, CO, CH_4 and lighter hydrocarbons and improves the lower heating value of syngas up to 28% and 43% for seed corn and wood, respectively. For all tested biomass feedstocks, results showed that ammonia and NO_X concentrations increase as the oxygen percentage in air increase. This, in turn, resulted in higher NO_X emissions during combustion.

Chapter 1 – Introduction

1.1 – The Needs for Green and Renewable Energy.

Energy has always been the foundation for growth in population, economics and technologies. Worldwide, fast growing population couple with evermore energy dependent technologies in the modern age indicates that energy consumption demands are expected to rise dramatically. Fossils fuels—natural gas, petroleum, and coal—has made up the majority contribution to the world energy supply system, however, fossil fuel reserves are finite and fast depleting.

Moreover, the usage of fossil fuels has led to the increasing emissions that are harmful to both human health and the environment. Therefore to avoid the energy crisis and reduction of the use of fossil fuels, considerable efforts and proactive decisions need to be made with respect to extracting and utilizing renewable energy resources.

In order to achieve the two goals, the feasible solutions are: 1) to improve the efficiency of existing fossil fuel conversion processes; 2) the use of renewable resources such as hydropower, geothermal, wind, solar, and biomass. Of the two options, the second option has additional advantages besides solving GHG emissions and petroleum fuels shortage. For example, the development and usage of renewable energy can help the government to develop national energy supply and become less dependence on foreign resources. Furthermore, renewable energy enhances economic development of rural areas.

1.2 – Biomass is an Important Part of Renewable Energy Sources.

Biomass, defined as any organic materials of recent biological origin (Brown, 2003), includes agricultural crop residues, forest residues, energy crops, organic municipal wastes (MSW), and animal wastes. Biomass has been the earliest energy resource gathered and utilized by humankind. Upon the discovery of fossil fuels during 19th and 20th centuries, the use of biomass as energy sources have been drastically declined (Biomass Technology Group, 2005). However, there has been a recent renewed interest in using biomass as energy sources driven by increasing global energy demands, coupled with diminishing of fossil fuel supplies. In addition, pressures from stringent regulations on air pollution and greenhouse gas emissions helps make biomass become even more attractive as environmental-friendly energy sources.

In 21st century, biomass is recognized as an attractive energy resource with 12 billion dry tons (equivalent to 270 EJ of energy content) available worldwide annually on sustainable basis (Walter et al., 2007). The current commercial and non-commercial biomass use for energy production is estimated to be between 6 and 17% of world primary energy. Most of this is used in developing countries where biomass accounts for up to one third of energy supplies. In developed countries, however, biomass is significantly made up of less energy needs. Figure 1 below depicts that in the United States, biomass has surpassed hydroelectric power and is currently the most important renewable energy resources.

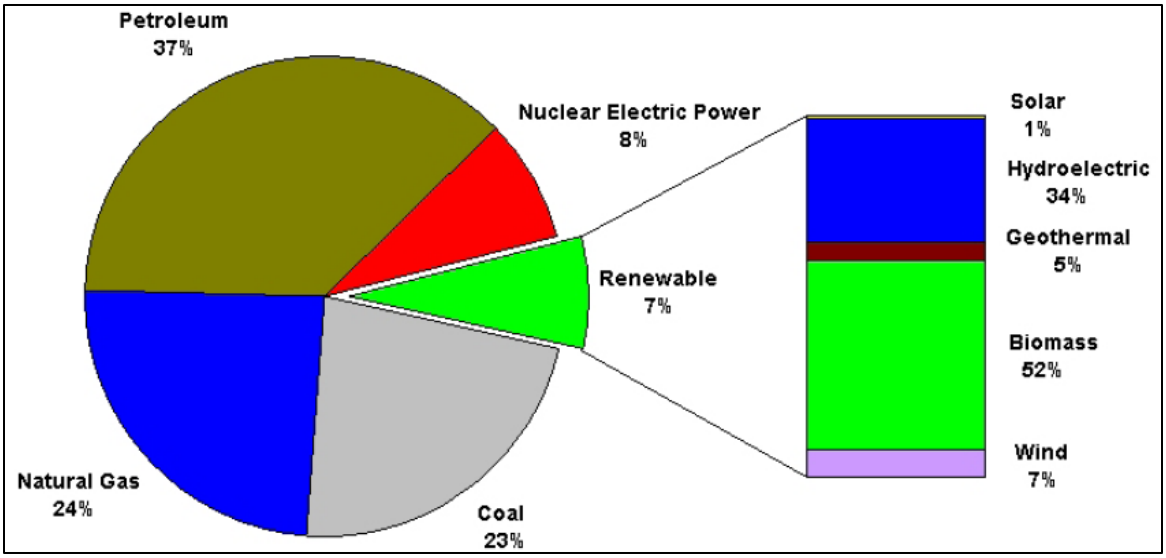

Figure 1: U.S. energy consumption in 2008.
Source: U.S. Energy Information Administration.

Unlike finite fossil fuels, biomass is clean, sustainable and is the only renewable hydrocarbon energy source (Nakanishi et al., 2010) that can fulfill the dual roles of substitution for fossil fuels and help mitigate global climate changes. For instance, through biochemical and thermochemical conversion processes biomass can be used to produce (Basu, 2010):

- Liquids (ethanol, biodiesel, methanol, vegetable oil, and pyrolysis oil).
- Gaseous (biogas (CH_4, CO_2), producer gas (CO, CO_2, CH_4, H_2, H_2O, N_2), syngas (CO, H_2), and substitute natural gas (CH_4)).
- Solids (charcoal, torrefied biomass)

The usages of these biomass products for chemical, heat and power, and transportation fuels have close to zero net carbon release to the atmosphere. This is because the fixed carbon in biomass when burned will be consumed as new biomass are plant and grow, thus their use does not add to overall atmospheric carbon. However, fuel and energy production from biomass

require energy inputs from fossil fuels during agricultural production and operation of equipment in the production plants thus result in non-zero net carbon cycle.

1.3 – Pros and Cons of Different Biomass Conversion Technologies

Although biochemical conversion technologies are well developed and most widely used for biofuels production (Basu, 2010), biochemical is not the most effective method in utilizing biomass resources. For example, production of biofuels (ethanol and biodiesel) from fermentation process is only possible with food crops (corn, sugarcane, wheat, barley, sorghum, etc.) as input feedstock. Consequently, this leads to the controversy of "Food vs. Fuel" debates as well as undesirable surges in food prices. Besides, fermentation is only feasible with large developed countries such as the U.S. where agricultural production exceeds the required food and animal feed needs. Thus there is an urgent need for technologies that can operate on both edible and non-edible biomass (wood, switchgrass, energy crops, MSW, and animal wastes) for production of biofuels with high efficiency.

Thermochemical gasification appears to be a promising technology that can exploit the embedded energy within various kinds of biomass and convert into valuable intermediates with flexibility for many industrial market applications such as heat, electricity and liquid fuels (Chen et al., 2007). Gasification turns solid biomass into low to medium heating value combustible gas mixtures through simultaneous occurrence of exothermic oxidation and endothermic pyrolysis under limited oxygen supply (Brown, 2003). The gas mixture is known as producer gas or syngas depending on the conditions run at the gasifier side. Typically, the term producer gas is used for air blown gasification whereas the term syngas is used for steam or oxygen blown

gasification. Because the study focuses on steam and oxygen gasification, syngas will be used throughout this article. Producer gas/syngas are comprised of hydrogen (H_2), carbon monoxide (CO), light hydrocarbons, water vapors, tars and solid chars.

Inherently, the gas mixture heating value and composition are greatly effect by the type of gasifying agents. Among gasifying agents, commercially the most widely used is air due to simplicity and low cost operations. Due to nitrogen dilution, air blown gasification typically yields product gas with heating value in the range of 4-7 MJ/Nm^3 which suitable for heat and power generation but not for uses of synthesis processes to produce valuable chemicals and liquid fuels (Gil et al., 1997). Air blown gasification has been studied by many researchers and is well-developed, thus will not be the focus of this study.

The use of pure oxygen as gasifying agent can produce medium heating value syngas (10-18 MJ/Nm^3) (Schuster et al., 2001) but high capital cost for oxygen production equipment has precluded this as viable for industrial scale. Steam is another interesting gasifying agent that can yield medium heating value (10-16 MJ/Nm^3) with H_2 rich gas (Ptasinksi et al., 2009). However, the process will become more sophisticate because indirect or external heat supply is needed for the endothermic reactions.

Although there are drawbacks, but steam and oxygen blown gasification are still being the subjects of many studies in order to improve syngas heating value and main combustible gas components such as H_2, CO, and CH_4 which are necessary for meeting market demands for power and liquid biofuels production. According to Kirkels and Verbong (2011), five major applications of over 100 MW_e electric equivalents capacity gasification plants are Fischer-

Tropsch, power generation (electricity), hydrogen, ammonia, and methanol of which Fischer-Tropsch and power generation are accounted for 29% and 24% of total capacity respectively.

Thus, adequate research has been done on biomass gasification using pure steam (Umeki et al., 2010), pure oxygen (Zhou et al., 2009), steam-air (Lv et al., 2004), and steam-oxygen (Gil et al., 1997), however there has been relatively little works done on oxygen enriched-air with steam (Campoy et al., 2009). Moreover, works from all these authors were focused only on increasing gas heating values and H_2/CO contents through different operating conditions but have not considered the effects of steam and oxygen on fuel-bound nitrogen (FBN) formation. High contents of FBN such as ammonia (NH_3), nitric oxide (NO), and hydrogen cyanide (HCN) in syngas have always been one of the most challenging aspects due to their significant contribution to high NO_x emissions for the use of gas in burners, boilers, and gas turbines for heat and power applications.

NO_x has adverse effects on both human health and environment. NO_x can cause irritation to the eye and throat, nausea and headache. When comes into contact with rain water droplets, NO_x decomposes and produce nitrous acid and nitric acid which contribute to acid rains that damage buildings, agricultural crops, and kill aquatic organisms. Likewise, NO_x can also react with volatile organic compounds (VOCs) under presence of sunlight to form smog (ground level ozone)—that can trigger millions of asthma attacks (Baukal, 2001). As mentioned earlier, there is an increasing tendency of utilizing syngas for heat and power generation. Thus there exists a strong need to quantify FBN concentration in syngas in order to achieve true zero-emissions

which would further enable the successful of implementation, commercialization, and competitiveness of biomass gasification technologies.

1.4 – Objectives

The purpose of this research is to investigate and provide fundamental understanding of the effects of using oxygen enriched-air and steam as gasifying agents on syngas composition, heating value, and formation and destruction of main NOx precursors—ammonia—during biomass gasification. In addition, this study also aims for characterization of NOx emissions from syngas combustion in an industrial burner at different operating conditions. This valuable information is then use to design burner that can effectively and cleanly burn biomass-derived gas. Burner design is out of scope of this study thus will not be discussed.

Chapter 2 – Literature Reviews

2.1 – Gasification History

Gasification is an old concept that was developed in the early 1800s and has greatly contributed to the early industrial development for production of gaseous fuel (known as town gas) used for heating and lighting purposes. Town gas cost was much cheaper compared to oil lamps, candles, and coal in heating and lighting applications. As a result, it was popular and spread quickly throughout Britain by 1859 (Basu, 2010). However, the use of electric light bulbs and natural gas in the 1900s substantially reduced the need of gasification in household and industrial applications.

During World War II, there was a renewed interested for gasification in Germany due to a shortage of liquid petroleum fuels. Consequently, many cars and trucks were powered by on-board small-scale gasifiers capable of utilizing both coal and biomass as feedstock. Furthermore, German scientists during this period also developed the Fischer-Tropsch process in which producer gas can be chemically synthesized into various liquid fuels (Brown, 2003).

Gasification technology was also employed in the United States in the 1950s. However, the technology was not widely commercialized until the 1970s and post 2000s in response to the "energy crisis" resulting from the Arab Oil embargo and mitigation of global climate change respectively. Since then, many financial incentives are provided by the U.S. government for further research and demonstrating the feasibility of gasification projects such as the Integrated Gasification Combine Cycle (IGCC) electric power plant. Today, gasification is a booming area.

There are many commercial developers conducting research on gasification technology and building high-tech power plants, utilizing biomass gasifiers to produce clean fuel (Biomass Technology Group, 2005).

2.2 – Gasification Process

The overall gasification process is endothermic which requires either simultaneous burning of part of the fuel or the delivery of an external source of heat to initiate the process. Primarily, solid biomass in the gasifier undergoes four steps in order to be decomposed into combustible gas (CO, H_2, CH_4, lighter hydrocarbons) in addition to solid chars, organic tars and inorganic contaminants (NH_3, HCL, H_2S): 1) heating and drying; 2) pyrolysis; 3) solid-gas reactions; 4) gas-phase reaction. The amounts of combustible gas, solid chars, liquid tars, and contaminants greatly depend on biomass characteristics, types of gasifiers, gasifying mediums, and operating conditions such as temperature, pressure, equivalence ratio, and residence time. A short description of gasification processes is given below.

- **Heating and Drying:** Initially, an external heat source is required to vaporize and dry the moisture in the biomass as well as raise the temperature to trigger the pyrolysis step. Alternatively, small amount of oxidant, air or oxygen, is introduced to the gasifier to combust portion of biomass to provide the heat required for subsequent endothermic reactions. According to Basu (2010), a minimum of 2260 kJ of energy from the gasifier is required to vaporize every kilogram of moisture in biomass. Therefore, raw biomass feedstock (moisture content can range from 30 to 90 weight percent) always needs to undergo a pre-drying step to achieve a moisture content of 10 to 20 percent in order not

to reduce the overall process efficiency and obtain moderate heating value in producer gas/syngas. Moisture evaporation occurs at temperatures from 100 to 150 °C.

- **Pyrolysis:** This process involves the thermal breakdown of large complex biomass molecules into smaller volatile gas molecules in the temperature range between 300 to 400 °C with negligible chemical reactions with the gasifying medium (Basu, 2010). The volatile gases include CO, CO_2, H_2, H_2O (steam), light hydrocarbons, and tars. Tar is a black viscous substance with a strong odor that consists of complex hydrocarbons with molecular weights higher than benzene. Tars are undesirable contaminants in gasification gas that need to be removed before downstream applications to avoid operational problems such as clogging up pipelines, valves, filters, and fuel injectors upon condensation (the boiling point of tar is around 80 °C). Tar is reactive with steam and oxygen, thus tar amounts decrease with an increase in oxygen and steam concentration. Moreover, increases in temperature also reduce tars through thermal cracking. In addition to volatile gases, solid chars are formed during the pyrolysis process. Char is the portion of biomass that remains as a result of incomplete reaction. Char mainly consists of carbons (about 85%) and lesser amounts of hydrogen, oxygen, nitrogen, and inorganic material referred to as ash (Pinto et al., 2009).

- **Gas-Solid Reactions:** This stage is also known as char combustion, flaming combustions, or oxidation zone. The volatile products and some of the char react with reactive chemical species (gasifying agent and other gases) in the surroundings to further produce gases (CO, H_2, and CH_4), tars, and ashes. This is an exothermic reaction step

where the heat produced from the oxidation reactions is used to drive the drying and pyrolysis processes. Note that the heterogeneous reactions between gas and solid char are relatively slow compared to pyrolysis stage and gas phase reactions and thus are considered to be the rate limiting in the gasification process (Biomass Technology Group, 2005).

- **Gas-phase Reactions:** This stage involves homogeneous reactions between gas phase species. The main chemical reactions are water-gas-shift, steam reforming, and methanation which includes the use of species such as water vapor, H_2, CO, and CH_4. This stage reduces the more reactive or thermodynamically unstable species and determines the final gas mixture in the gas product (thus sometimes is referred to as reduction zone). The final gas product is a strong function of type and amount of oxidants introduced to the reactor as well as residence time and temperature of reaction (Pinto et al., 2009).

2.3 – Gasification Reactors

Various gasifier designs have been developed. The three main gasifiers that are of interest in biomass gasification are: updraft gasifier, downdraft gasifier, and fluidized bed gasifier. Differentiation between gasifiers is based on the means of supporting biomass in the reactor, direction of both biomass and oxidant, and the way heat is supplied to the reactor. The choice of gasifier depends on type of biomass (sizes, moisture and ash contents), output capacity, and gas quality.

A brief description of each type of gasifier is given below. In addition, Table 2.1 summarizes the advantages and disadvantages of the three gasifiers. Note that updraft and downdraft gasifiers are so-called fixed bed gasifiers in which feedstock move either concurrent or countercurrent to the flow of gasifying medium as chemical reaction takes place and the feedstock is converted to gases. Fixed beds are primarily suited for solid fuel contacting operations that require close temperature control, carryover of particles away from the reaction zone, simple operations and minimum erosion of the body of the reactor.

2.3.1. – Updraft Gasifier

This gasifier is also known as countercurrent gasifier. This is the simplest and oldest gasifier design. In this system, gasifying agent is introduced from the bottom of the reactor and feedstock is introduced from the top. As it comes down, the feedstock passes through the drying zone, pyrolysis zone, reduction zone, and oxidation zone. The gasifying agent first passes through the grate (used as reactor support) at the bottom of the reactor and diffuse up through the bed fill with feedstock. The gas tends to leave the gasifier at low temperatures due to combustion taking place at the bottom of the gasifier. Low temperatures are favorable for tar formation, and in order to reduce tars, gasifier temperature needs to be maintained at about 850 °C. The hot combustion gas (CO_2 and H_2O) is cooled as it moves upward the reactor and reacts with char to produce H_2 and CO. Continuing up the reactor, the reducing gases pyrolyze the dry descending biomass and finally dry the incoming wet biomass, thus leaving the reactor at low temperature, ~ 500 °C (Brown, 2003).

2.3.2 – Downdraft Gasifier

This gasifier is also known as concurrent gasifier. This design is virtually the same as the updraft gasifier except that both biomass and gasifying medium are introduced to the reactor in the same direction. The feedstock also undergoes four different gasification zones but in slightly different order (drying, pyrolysis, oxidation, and reduction). Opposed to the updraft gasifier, the product gases leave the reactor at the combustion zone, thus exiting at higher temperatures (around 800 °C). This results in an increased hydrogen concentration and very low tars, making it an ideal fuel for combustion engines (Brown, 2003).

2.3.3 – Fluidized Bed Gasifiers

Contrary to fixed bed reactors, different reaction zones cannot be distinguished in fluidized bed reactors. This is due to the intense mixing between feedstock and gasifying agent which facilitates simultaneous reactions within the reactor. The turbulence in the reactor promotes uniform bed temperature and enhances the heat and mass transfer which lead to increases of reaction rates and carbon conversion efficiency (up to 97%). Typically, fluidized beds are designed for large-scale and high capacity gasification (greater than 10 MW_{th}) applications. Two primary fluidized bed designs are bubbling fluidized bed and circulating fluidized bed (Biomass Technology Group, 2005).

1. Bubbling Fluidized Bed Gasifier

Bubbling fluidized bed reactors can be divided into two sections: dense phase and freeboard. The dense phase is consisted of fluidizing medium (inert particles such as sands and limestone) and feedstock. The freeboard section is the area above the dense phase that decreases syngas

velocity to facilitate the separation of syngas from bed media, large char particles, and biomass (Evans et al., 2010).

Gasifying agent is introduced through the bottom of the reactor with a velocity great enough to overcome the gravitational force exerted by inert bed particles. At this point the particles are levitated and become suspended. This gas velocity is known as minimum fluidization velocity, U_{mf}. When the gas velocity is further increased, the bed begins to bubble and initiate turbulent mixing behavior similar to that of a continuously stirred reactor. Achieving an optimum fluidization velocity is important in designing fluidized bed reactors. If the velocity is too low, fluidized motion will not occur. When the velocity is too high, syngas along with bed media, large char particles, and biomass will be entrained out of the reactor (Timmer, 2008).

Feedstock is often fed via screw feeding mechanism into the reactor (when the desired temperature is reached) where it is rapidly dried and pyrolyzed upon coming to contact with the hot fluidizing bed. The remaining char particles further react and gasify until they are small enough to be suspended in syngas in the freeboard and carried out of the reactor. To achieve high carbon conversion, feedstock is usually fed near the bottom of the hot bed in order to lengthen the residence time.

The major advantage of this system is that the hot fluidized media breaks up the feedstock fed into the bed thus enabling homogeneous mixing, good heat and mass transfer between solid and gas, and better temperature control. Moreover, the bubbling fluidized bed permits addition of

catalysts such as nickel, alkali metals, dolomite, olivine or alumina to reduce contaminants and improve quality of syngas for suitable end applications (Pinto et al., 2009).

2. Circulating Fluidized Bed Gasifier

Circulating fluidized bed (CFB) shares similar reactor design, advantages, and operating concepts as bubbling fluidized bed. In both designs, feedstock is immediately mixed with bed media and gasifying agent once introduced into the bed. The main difference is that circulating fluidized bed has no distinct interface between dense phase and freeboard (Biomass Technology Group, 2005). In this system, the fluidization velocity (3.5-5.5 m/s) is much higher than of bubbling bed (0.5 to 1.0 m/s) which continuously pushes and circulates the bed materials and ungasified solid particles (feedstock and chars) between the reactor and a cyclone separator. The solid particles separated from syngas by the cyclone are recycled back to the reactor for further gasification. Thus CFB has longer gas residence time and higher char conversion compared to bubbling bed which makes it ideal for high volatile fuels such as biomass.

Table 2.1: Pros and Cons of Gasifiers

Type of Gasifier	Advantages	Disadvantages
Updraft	• Simple and inexpensive • High gasification efficiency • Can handle high moisture (up to 60%) • No carbon in ash	• Feedstock size limits • High tar yields ~ 50/m^3 • Very sensitive to tar and moisture content of feedstock
Downdraft	• Small scale application • Low tars • Low particulates • Low power requirement	• Feedstock size limits • Feedstock moisture content limits (less than 30%) • Scale limitation (max capacity ~ 400 kg/hr
Fluidized Bed	• Easily scaled to large size for power & electric production • High heat rate and mass transfer • Fuel flexibility - wide variety of biomass with high moisture content and small size	• Higher power requirement • Higher capital cost • Medium tar yield ~ 10 g/m^3 • High particulate in the gas

2.4 – Gasification Reactions

The global biomass gasification reaction can be represented by the following generic equation:

$$CH_xO_y + O_2 + H_2O(steam) \rightarrow CH_4 + CO + CO_2 + H_2 + H_2O(unreacted\ steam) + C(char) + tar + contaminants \quad (2.1)$$

A series of simultaneous homogeneous and heterogeneous reaction steps and pathways occur before the product gas can reach its final composition.

2.4.1 – Heterogeneous Reaction

Heterogeneous reactions are reactions that arise from char particles with gasifying agent as well as reaction between char particles and volatile gases. The main heterogeneous reactions and standard enthalpy change are:

$C_s + \frac{1}{2}O_2 \rightarrow CO$ -111 kJ/mol (2.2)

$C_s + O_2 \rightarrow CO_2$ -394 kJ/mol (2.3)

$C_s + 2H_2 \leftrightarrow CH_4$ -74.8 kJ/mol (2.4)

$C_s + CO_2 \leftrightarrow 2CO$ +172 kJ/mol (2.5)

$C_s + H_2O \leftrightarrow H_2 + CO$ +131 kJ/mol (2.6)

The first two equations are combustion reactions that occur in the oxidation zone. These two reactions provide the heat necessary for the endothermic reactions and sustain the gasification process without addition of heat from an external source (Brown, 2003). The latter three reactions increase the gas yield of CO and H_2 at high temperature and low pressure. Also, these equations show that solid carbon can react with different gasifying agents (i.e. steam, O_2, and CO_2) and form simpler gas molecules such as CO and H_2.

The Boudouard reaction Eq. (2.5), involves the gasification of carbon with CO_2. This reaction has three steps and the reaction rate is several orders of magnitude slower compared to the combustion reactions. Gasification of char in the presence of steam is represented by Eq. (2.6), the water-gas reaction. This reaction is also slower than the combustion reactions, however, it is

faster compared to the Boudouard reaction. The relative carbon conversion rate is as follows (Basu, 2010):

$$R_{C+O_2} \gg R_{C+H_2O} > R_{C+CO_2} \gg R_{C+H_2}$$

2.4.2 – Homogeneous Reaction

Homogeneous reactions are reactions that occur among volatile gases (released during pyrolysis) as well as reactions between volatile gases and gasifying agent. Homogeneous reactions are relatively simple and fast compared to heterogeneous reactions. Moreover, many of these gas phase reactions can achieve chemical equilibrium at the operating temperature and pressure of gasifiers (Liu et al., 2010). The following gas phase reactions take place in a gasifier where the rate of each reaction is heavily dependent on the choice of gasifying agent and operating conditions:

$CO + H_2O \leftrightarrow CO_2 + H_2$	-41.2 kJ/mol	(2.7)
$CO + 3H_2 \leftrightarrow CH_4 + H_2O$	-206 kJ/mol	(2.8)
$2CO + 2H_2 \rightarrow CH_4 + CO_2$	-247 kJ/mol	(2.9)
$CO_2 + 4H_2 \rightarrow CH_4 + 2H_2O$	-165 kJ/mol	(2.10)
$CO + \frac{1}{2}O_2 \rightarrow CO_2$	-284 kJ/mol	(2.11)
$H_2 + \frac{1}{2}O_2 \rightarrow H_2O$	-242 kJ/mol	(2.12)
$CH_4 + 2O_2 \leftrightarrow CO_2 + 2H_2O$	-803 kJ/mol	(2.13)

These reactions are exothermic reactions and therefore raise the overall product gas temperature and provide heat to drive the gasification process. However, oxidation reactions from equations 2.11 to 2.13 have an adverse effect on the gas heating value. Equations 2.7 and 2.8 are referred to as water-gas shift and methanation reactions respectively. In a bubbling fluidized bed reactor, these are the only two main reactions that occur in the freeboard of the reactor since all the oxygen is consumed in the lower region of the bed. These two reactions contribute to the increase in gas heating value since CH_4 and H_2 have a high heat of combustion. The water-gas shift is a very important reaction since it affects the H_2/CO ratio in the product gas which determines the appropriateness for gas upgrade using synthesis processes.

The generated CO_2 and H_2O molecules (as well as the unreacted molecules that escaped from the bed) can undergo heterogeneous endothermic reactions with chars and tars that entrained with product gas to the freeboard. According to Timmer (2008), the CO_2 and H_2O reaction rates with char-carbon is approximately five orders of magnitude slower compared to carbon-oxygen reactions and the H_2O reaction rate is 4 to 100 times faster than CO_2 reaction rates. Notice that Eq. (2.8) is a reversible reaction, therefore when steam is used as a gasifying agent, additional H_2 can be generated. The reverse reaction is referred to as the steam reforming reaction.

2.5 – Influence Factors on Gas Composition and Quality

Biomass-derived gas composition from gasification is affected by various factors such as, but not limited to, type of feedstock, gasifier designs, operating conditions, and gasifying media. Therefore, large variation of gas compositions can be expected. Different end-gas applications call for certain syngas compositions (especially the H_2/CO ratio) and tolerate different amounts

of gas contaminants. Therefore the purpose of the following section is to address the effects of some important factors on the product gas composition and contaminants.

2.5.1 – Effects of Feedstock

Compared to coal, biomass has higher volatile content and higher char reactivity (70-90 wt% for biomass and 30-40 wt% for coal). This makes biomass the ideal raw materials for gasification. When using biomass for heat and energy production, the most important factor needed to be considered is the moisture content. Biomass has consistently higher moisture content compared to coal or petroleum which translates to a much lower heating value (Brown, 2003). In addition, the high oxygen content causes biomass to have less energy density compare to coal.

Because biomass feedstock elemental compositions are not homogeneous, the final gas product obtained from different feedstock can have a wide degree of variability even when gasified at similar experimental conditions. This effect is illustrated in an experimental study conducted by Pinto et al. (2009). In the study, five different types of biomass with different CHNOS compositions were gasified at the same conditions and gas composition distribution such as CO, CO_2, H_2, CH_4, light HC's, NH_3, H_2S, and tars were observed to be varied. For example, pine has the second lowest carbon content but produced highest CO concentration. Another important trend showed by the study was that feedstock with higher nitrogen content resulted in higher ammonia concentration in syngas. The direct relationship between nitrogen content in feedstock to ammonia concentration in syngas was also reported by Yu et al. (2006).

There are three different methods widely used for evaluating biomass characteristics of interest for gasification: proximate analysis, ultimate analysis, and organic compound analysis. Ultimate analysis can be performed either on a wet or dry basis. On the wet basis, moisture is reported together with elemental composition such as C,H,N,O,S by wt% where H and O do not include the hydrogen and oxygen atom in the moisture. Dry basis, on the other hand, incorporates the H and O atoms present in the moisture into H and O atoms in the organic part of biomass. Proximate analysis gives composition of biomass in terms of volatiles, moisture, fixed carbon, and ash. This method is relatively easy and inexpensive compared to ultimate analysis. Organic compound analysis breaks down and reports the content of organic structures of biomass: cellulose, hemicelluloses, and lignin. More detailed descriptions of each method can be found in Basu (2010).

2.5.2 – Effects of Operating Conditions

Similar to biomass feedstock, operating conditions have major impacts on the overall gas composition and quality. Operating conditions need to be optimized so that residence time and heating rate are adequate to achieve high carbon conversion and thermal cracking of tars so that higher gas yields, higher process efficiency, and lower gas contaminants can be achieved.

2.5.2.1 – Effect of Equivalent Ratios

In gasification industry, the equivalence ratio (ER) is defined as the ratio of actual air-fuel ratio to the stoichiometric air-fuel ratio. This definition is opposed to that used in combustion analysis. The stoichiometric air-fuel ratio can be computed using the ultimate analysis of the feedstock. ER greater than one indicates that excess air is supplied and the condition is lean.

Whereas ER less than one means deficient air supply and the condition is rich such that gasification occurs.

In gasification, it is widely accepted that the optimum ER is between 0.2 and 0.3, i.e. air supply is only 20 to 30% of its stoichiometric requirement. Even though higher ER offers higher carbon conversion efficiency, too high of ER (greater than 0.4) will have adverse effects of oxidizing part of the fuel gas and will result in excessive complete combustion products (CO_2 and H_2O) which lower the gas heating value. On the other hand, too low of ER (less than 0.2) gives high content of tars and chars. This is because of insufficient oxygen for complete gasification of carbon which leads to lower gasification bed temperature for thermal cracking of tars (Basu, 2010).

Timmer (2008) reported that there is a direct positive relationship between increasing ER and increasing gas-solid reaction rate. The experiments were conducted on a lab-scale bubbling fluidized bed reactors using discarded seed corn as biomass feedstock. The range of ERs tested is from 0.27 to 0.34 at 750 °C and 0.24 to 0.37 at 800 °C. The increase in gas-solid reaction rate indicates higher carbon conversion efficiency, thus lower char contents. There were no data on the effect of increasing ER on tars production.

According to Biomass Technology Group, the optimum ER for biomass gasification is approximately 0.25. At ER of 0.25, the CO concentration is peaked which shows that all the char is gasified and converted into gas. Also, at this point the gas heating value should be

highest due to lowest CO_2 concentration. Beyond 0.25, CO_2 and H_2O concentration increase at the expense of decreasing CO and H_2 concentration.

2.5.2.2 – Effect of Temperature

Increasing gasification temperature is favorable for carbon conversion efficiency as it increases the gas-solid reaction. Moreover, increases in temperature promote thermal cracking of tars and reactions with O_2 and H_2O (Pinto et al., 2009) as well as enhancing the endothermic reaction between solid carbon and volatile gases (i.e. CO and CH_4) with steam to increase H_2 and CO gas yields. According to Kumar et al. (2009), H_2 yields are more favorable at temperatures between 750 to 800 °C through water-gas shift and steam reforming reaction whereas CO yields are dominate at temperatures above 850 to 900 °C through steam reforming and Boudouard reactions.

2.5.3 – Effects of Gasification Media

Gasifying media or gasifying agents include, but are not limited to: air, steam, oxygen, or combination of them. The choice of the gasifying agent has direct effects on product gas composition distribution and gas heating value and the choice is determined by the desired composition of end-product. Air gasification is the simplest and least expensive of all gasifying agents, however, the trade-off is low gas energy density due to dilution presence of nitrogen in air. Steam gasification is gaining attention due to the possibility of increasing product gas H_2 content from hydrogen molecules in steam. However, steam gasification is highly endothermic thus high external heat supply and complex circulating systems have to be implemented in order or achieve autothermal process. The use of pure oxygen is very beneficial to carbon conversion

efficiency and increases the gas heating value but production of oxygen from air separation is very expensive. Thus many researchers (Gil et al., 1996; Lv et al., 2003; Campoy et al., 2009) have explored the use of air-steam mixture, oxygen-steam mixture and oxygen-enriched air as gasification mediums.

Typical gas compositions obtained from different gasifying agents are outlined below:

1. Experiments were conducted by Gil, et al. (1999) using atmospheric bubbling fluidized bed reactor to compare gas production distribution between the use of air, pure steam, and steam-oxygen mixture. The biomass feedstock used is pine wood chips.

Table 2.2: Effects of Different Gasifying Agents on Gas Composition.

	Air	Steam	Steam-Oxygen
Operating Conditions			
ER	0.18-0.45	0	0.24-0.51
Steam/Biomass (kg/kg)	0.08-0.66	0.53-1.11	0.48-1.11
T (°C)	780-830	750-780	785-830
Gas Compositions			
H_2 (vol%, dry basis)	5.0-16.3	38.0-56.0	13.8-31.7
CO (vol%, dry basis)	9.9-22.4	17.0-32.0	42.5-52.0
CO_2 (vol%, dry basis)	9.0-19.4	13.0-17.0	14.4-36.3
CH_4 (vol%, dry basis)	2.2-6.2	7.0-12.0	6.0-7.5
C_2H_n (vol%, dry basis)	0.2-3.3	2.1-2.3	2.5-3.6
N_2 (vol%, dry basis)	41.6-61.6	0	0
Steam (vol%, wet basis)	11.0-34.0	52.0-60.0	38.0-61.0
Tars (g/kg)	3.7-61.9	60-95	2.2-46
Char (g/kg)	n/a	95-110	5.0-20.0
Gas Yield (Nm^3/kg)	1.25-2.45	1.3-1.6	0.86-1.14
LHV (MJ/Nm^3)	3.7-8.4	12.2-13.8	10.3-13.5

As Table 2.2 shows, the gas composition distribution and heating values vary greatly with different gasifying agents. There is a noticeable increase in H_2 content when steam was used as gasifying medium whereas the highest increase in CO content occured with steam-oxygen mixture. These results agreed with Kumar et al. (2009) about the H_2 production dominance at temperature range between 750 to 800 °C through water-gas shift and steam reforming reactions. The dominance of CO concentration at steam-oxygen mixture is due to more availability of oxygen radicals to react with carbon in solid char particles (the oxygen radicals are contributed from both oxygen itself and the breakdown of steam to OH and O radical at high temperature). This is confirmed when examining char yields between steam only and steam-oxygen mixture gasification. Char yield is higher in pure steam gasification compared to steam-oxygen mixture gasification. This is due to higher reaction rate between carbon-oxygen compared to carbon-steam as mentioned in Section 2.4.1.

2. Biomass air-steam gasification experiment in an atmospheric fluidized bed reactor was conducted by Lv et al. (2004) to investigate the effects of some of the important factors (ER, reactor temperature, and steam-to-biomass ratio) on gasification performance. The biomass feedstock was pine sawdust. Two electrical heaters were installed around the reactor to supply initial startup heat and counter heat loss during operation. Air and steam were supplied at 65°C and 154 °C respectively. Although the author did not mention, however, it is believed during the experiments the two electrical heaters were supplying heat to increase the reactor temperature at constant ER as well as to counter the heat loss to environment and maintain constant reactor temperature at increasing ER.

According to the authors, H_2 is the only specie that increases at increasing temperature while gases such as CO, CH_4, and other HCs show opposing trends. Increases in temperature also favor and increase the reaction rates of water-gas shift and steam-reforming reaction. Thus H_2 concentration increases as CO and CH_4 concentrations decrease. Table 2.3 shows that the percentage of steam decomposition increases with increasing reactor temperature. This further indicates that there are strong reaction between steam-CO and steam-CH_4 to form H_2. The experimental results also showed that there is a steep decrease in CO concentration while CH_4 concentration shows little decrease. This illustrates that the reaction between steam-CO is stronger compared to steam-CH_4. In this experiment, the CO concentration shows an inverse trend compared to CO concentration in steam-oxygen gasification conducted by Gil et al. Similarly, the CO production is not favorable at increasing temperature while in Javier et al.'s steam-oxygen experiment, the CO concentration increases with increasing temperature. One possible explanation is due to low ER of 0.22 (compare to ER of 0.24 and 0.55 in Gil. et al. experiment) there wasn't sufficient oxygen available to completely react with carbon in char particles.

Table 2.3: Experimental Results at Different Reactor Temperature.

Reactor Temperature (°C)	700	750	800	850	900
Biomass feed rate (kg/h)	0.445	0.445	0.445	0.445	0.445
Steam flow rate (kg/h)	1.2	1.2	1.2	1.2	1.2
Steam/Biomass	2.70	2.70	2.70	2.70	2.70
Air flow rate (Nm^3/h)	0.5	0.5	0.5	0.5	0.5
ER	0.22	0.22	0.22	0.22	0.22
Gas Yield (Nm^3/kg biomass)	1.43	1.51	2.23	2.45	2.53
LHV (MJ/Nm^3)	7.945	7.651	8.560	8.223	7.362
Carbon Conversion Eff. (%)	78.17	80.66	85.9	92.35	92.59
Steam Decomposition (%)	16.85	18.95	29.08	32.84	33.09

Furthermore, Lv et. al. experimental results showed that there is very little effect on gas composition with changing ER while holding reactor temperature constant. The CO concentration increases until ER of 0.23 and then decreases afterward. This is because more oxygen available for oxygen-carbon reaction when ER increases, however, when ER increases pass 0.23, oxidation reaction occurs therefore CO concentration decreases and CO_2 concentration increases. The increase and decrease of CO concentration is well correlate to the increases and decrease of gas lower heating values indicated in Table 2.4.

Table 2.4: Experimental Results at Different ER and Fixed Reactor Temperature.

Reactor Temperature (°C)	800	800	800	800	800
Air flow rate (Nm^3/h)	0.5	0.55	0.6	0.65	0.7
Biomass feed rate (kg/h)	0.512	0.512	0.512	0.512	0.512
ER	0.19	0.21	0.23	0.25	0.27
Steam flow rate (kg/h)	0.8	0.8	0.8	0.8	0.8
Steam/Biomass	1.56	1.56	1.56	1.56	1.56
Gas Yield (Nm^3/kg biomass)	2.13	2.25	2.37	2.18	1.88
LHV (MJ/Nm^3)	8.817	8.839	8.708	8.164	7.277
Carbon Conversion Eff. (%)	76.26	84.49	90.6	84	70.6
Steam Decomposition (%)	48.36	50.66	52.67	47.76	40.41

3. In this experiment, the concept of oxygen-enriched air mix with steam is proven as a possible gasifying agent for biomass. The experiments were conducted on a bubbling fluidized bed reactor using wood pellets as feedstock. The oxygen percent in air (OP), steam-biomass ratio (S/B), and ER were varied from 21% (v/v) to 40% (v/v), 0 to 0.63, and 0.24 to 0.38 respectively in order to find the optimum gasification condition that gives highest H_2 concentration CO, highest gas LHV, and highest carbon conversion efficiency. The inlet gasifying agent mixture was kept at 400 °C for all runs.

An experimental matrix of sixteen different test runs were constructed based on four values of OP (21, 30, 35, 40 %v/v) and two levels of ER and S/B, representing low and high values: 0.24-0.27 (low ER) and 0.33-0.38 (high ER) and 0.22-0.36 (low S/B) and 0.43-0.63 (high S/B). These tests can be grouped into four different combinations on the basis of the level of the ER and S/B ratio used. See Table 2.5 below for clarification.

Table 2.5: Effects of Different ER, S/B, and OP (Campoy et al., 2009)

Combination	1	2	3	4	1	2	3	4	1	2	3	4	1	2	3	4
Bed Temperature (°C)	804	789	786	755	808	790	781	765	820	795	800	757	829	806	803	766
Freeboard Temperature (°C)	721	709	708	709	715	715	16	695	715	725	725	720	708	727	725	722
OP (%)	21	21	21	21	30	30	30	30	35	35	35	35	40	40	40	40
ER	0.33	0.33	0.27	0.27	0.36	0.35	0.25	0.24	0.38	0.34	0.27	0.26	0.33	0.33	0.26	0.24
S/B	0.22	0.45	0.23	43	0.32	0.6	0.31	0.58	0.33	0.56	0.31	0.63	0.29	0.57	0.3	0.56
CO (%v/v, dry)	15.4	13.8	15	11.9	18.9	15.7	20.8	15.3	20	17.5	23.9	19.3	25.1	19.3	28.5	23.5
H_2 (%v/v, dry)	11.9	13.3	14	16.2	16.4	18.3	20	22.3	17.5	21.8	22.4	25.1	23.1	25.7	25.7	27.5
CO_2 (%v/v, dry)	15.9	17	16.2	18.6	17.6	18.8	15.8	2.3	16.8	18	12.6	16.2	13.7	17	9.2	14.6
CH_4 (%v/v, dry)	4.8	4.6	4.7	5.3	5.5	5.7	6.7	7.1	5.6	6.1	6.3	7.4	6.5	6.7	8.1	7.7
CO (g/kg)	443.4	402.7	365.7	302.8	456.1	362.8	405	305.6	475.1	366.1	438.1	3699.3	499.4	384.7	476.2	391.5
H_2 (g/kg)	24.5	27.7	24.4	29.4	28.3	30.1	27.8	31.9	29.7	32.6	29.4	34.3	32.9	36.6	30.8	32.7
CO_2 (g/kg)	719.3	779.6	620.6	743.7	669.7	681.6	482	639.3	626.7	591.5	361.8	487	427.6	532.7	242	381.3
CH_4 (g/kg)	79	76.7	65.5	77.1	76	75.1	74.5	81.2	76.1	72.9	76.5	80.7	73.9	76.2	77.5	73.2
Gas Yield (Nm^3 dry gas/kg)	1.11	1.14	0.97	1.06	1.13	1.08	0.98	1.04	1.14	1.06	0.97	1.04	1.09	1.1	0.96	0.98
LHV (MJ/Nm^3 dry gas)	4.95	4.83	5.09	5.15	6.12	6	7.19	6.88	6.41	6.75	8.06	7.81	8	7.62	9.28	8.7
Carbon Conversion (%)	90	92	90	91	94	95	96	96	95	95	96	96	96	96	97	97

Figure 2.1 and Figure 2.2 show H_2 and CO concentrations in product gas as function of oxygen percentage in air for different ER and steam-to-biomass ratios. Figure 2.1 shows that for all values of ER and S/B ratios, the CO concentration increased as OP increased. The highest CO production is shown by combination 3, low ER (0.25-.27) and S/B ratio (0.23-0.31). This is because at lower ER less CO is being consumed through oxidation reactions.

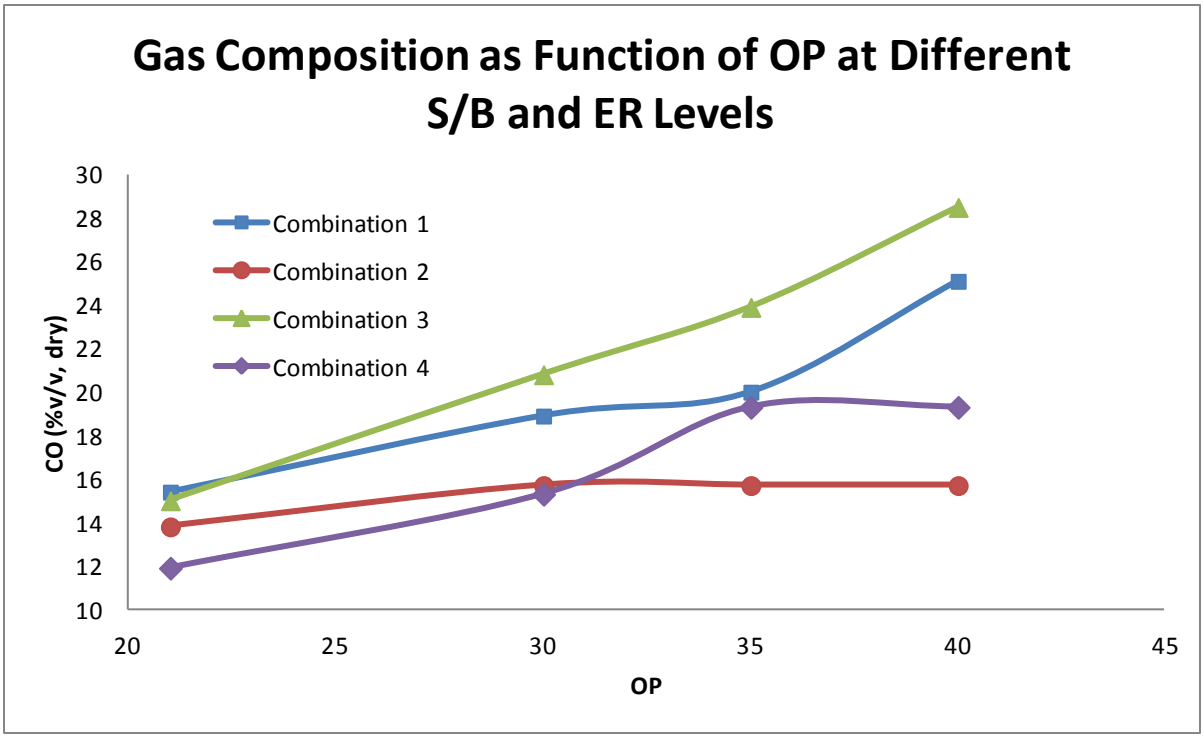

Figure 2.1: CO concentration as function of OP for different S/B and ER (Campoy, 2009).

Figure 2.2 shows the H_2 concentration in the gas. Similar with CO concentration, H_2 increased as OP level increased for all ER and S/B ratios. Combination 4, low ER (0.24-0.27) and high S/B ratio (0.43-0.63), shows the highest H_2 concentration increased. The increased in H_2 is attributed to the increased of OP at high S/B ratio. The increased in OP supplied more oxygen to facilitate higher reaction rates for exothermic reactions which raised the bed temperature high enough to cracked steam and created more H_2—increased in temperature due to increase in OP can be seen in Table 2.5.

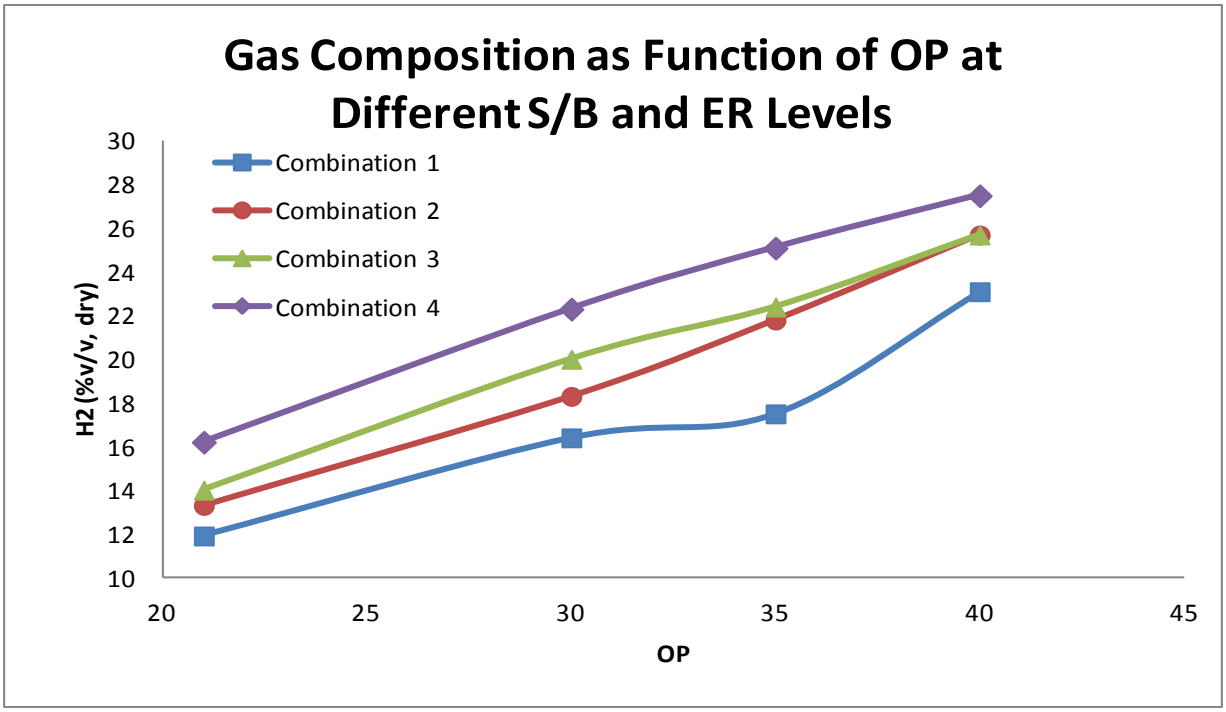

Figure 2.2: H_2 concentration as function of OP for different S/B and ER (Campoy, 2009).

Chapter 3 – Experimental Setups

3.1 – Introduction: Experiment Facility

Experimental research was conducted at BECON (Biomass Energy Conversion) facility located at Nevada, Iowa. The facility is the property of Iowa Energy Center established for housing and giving supports to several projects regarding various processes and technologies for converting solid biomass into clean and renewable energy. A project collaboration between Department of Mechanical Engineering at Iowa State University and Frontline BioEnergy was established to conduct studies on the feasibilities of converting different types of biomass into low to medium heating values gas using gasification—a thermochemical process. Moreover, ISU was aiming for the assessment of combustion performance of biomass derived gas in an industrial burner in order to develop strategies and possible new burner design to reduce overall NO_x emissions.

Figure 3.1: Biomass Energy Conversion Center at Nevada, IA.

3.2 – Gasification System

Figure 3.2 shows a schematic diagram of the demonstration pilot scale gasification and combustion systems. Tests were performed using a pressurized (up to 50 psig), directly heated bubbling fluidized bed gasification system, with air and air-steam-oxygen mixture as the

gasifying agent. The gasification system consists of a biomass feeding system, oxygen system, steam generation unit, fluidized bed reactor and gas cleanup components (baghouse and cyclone). The system is rated at 800 kW thermal inputs which correspond to feeding rate of 180 kg/hr of fuel with average value of heating value of 1600 kJ/kg.

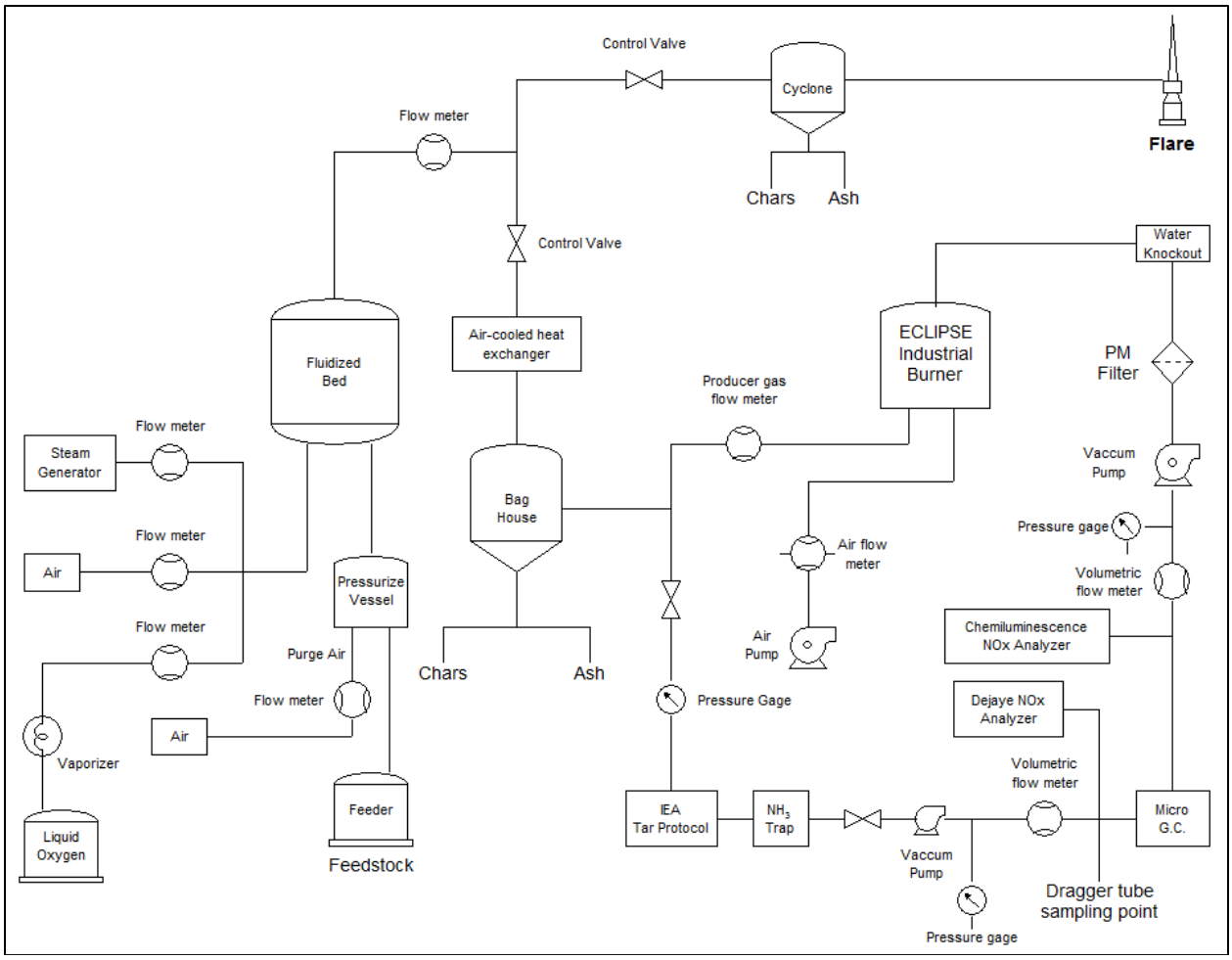

Figure 3.2: Schematic of biomass gasification and combustion system.

Biomass feeding system has three parts—feeding hopper and two pressurized vessels. Pelletized biomass are first loaded into the feeding hopper and then transported to a vessel at atmospheric pressure using a feed auger. The feeding auger, shown in Figure 3.3, is screw operated that feeds

the biomass into the vessel at constant rpm. The diameter of the screw feeder limited maximum size of biomass to a diameter of one inch.

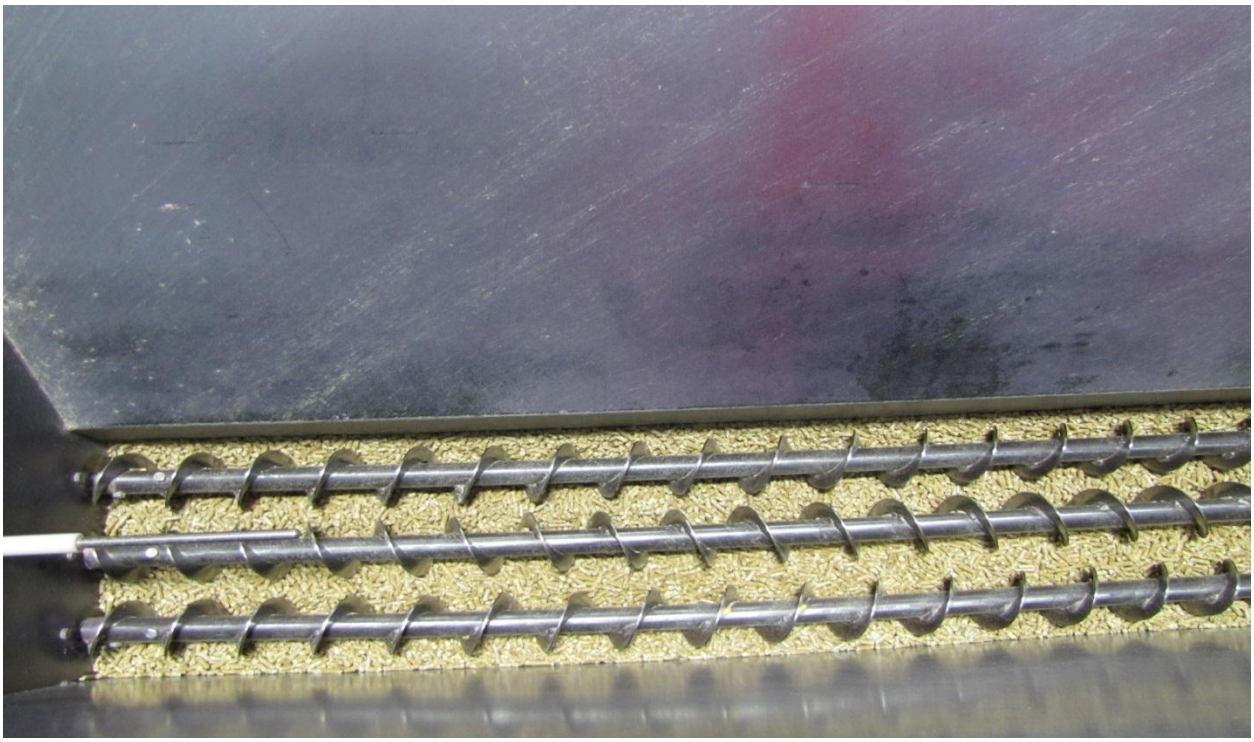

Figure 3.3: Feeding auger with screwed operated mechanism.

Once the first vessel is full, it is pressurized to 15-18 psig and the biomass is transferred to another pressurized vessel via same pressure and feeding mechanism. Finally, biomass is then introduced into fluidized bed reactor. Fluidized bed temperature is continuously monitored using four K-type thermocouples. The bed temperature for all experiment conditions is kept at approximately 800 °C. The fluidized bed has a bed depth of 1-1.3 m and is operated under pressure varying between 10-20 psig to achieve and maintain optimum fluidizing velocity. The fluidized bed reactor inner wall is surrounded by refractory lining in order to minimize heat loss to surroundings. At the bottom of the reactor, there are always present of silica sands and

limestone. Silica sands are used as fluidizing medium whereas limestone is used to prevent bed allogmeration and reduce tar formation.

Figure 3.4: Bubbling fluidized bed reactor column.

During gasification, air is purged into the second pressurized vessel in order to prevent backflows of combustible syngas from reactor which can causes explosion when comes to contact with biomass feedstock.

The oxygen system comprised of liquid oxygen storage tank with capacity of 1500 gallons. The system is designed for operating duration of 72 hours (at 2500 SCFH max flow of oxygen gas)

with blend of oxygen and air up to 90% oxygen purity. Liquid oxygen in the tank is at -400 °F (-204 °C) therefore safety barriers such as fence and bollards are built surrounding the tank. During operation, liquid oxygen passes through a vaporizer at 250 psig and converts to gas phase. The gas phase oxygen is then pass through the gas flow meter at 100 psig and ambient temperature to mix with air and steam before entering fluidized bed reactor.

Figure 3.5: Liquid oxygen system.

Before each experiment, the gasifier is warmed up overnight with preheated air (using electric circulating air heater) at approximately 538 °C. Next, low flow (40 lbs per hour) of biomass is fed into the gasifier and operated in combustion mode for several hours. During this time the reactor is operating at about 840-870 °C in combustion mode while all the downstream

equipment is warming to at least 316 °C to prevent tar condensation (on pipes between baghouse, cyclone, and fluidized bed reactor) when switching to gasification mode. When all desired temperature are established, biomass feed rate is increased to reduce air to fuel ratio for transition from combustion to gasification. After air gasification mode is established, the transition to oxygen enriched mode begins. This usually takes 10-15 minutes to reach steady state condition—when system temperature becoming stable. The transition is a simultaneous reduction of air flow, increase of oxygen and steam flows to achieve the desired level of oxygen operation. Steam is generated using a boiler with natural gas as fuel. Air-oxygen-steam fluidizing agents are well mixed before entering the fluidized bed reactor as single stream. Control systems are established for air, oxygen, and steam in order to monitor, record, and control the desire flow rates.

Hot syngas exiting fluidized bed reactor needs to go through gas cleaning stage (baghouse) to knock out solid residues such as chars and ash before sampling for gas composition analysis and entering burner for combustion. Baghouse is essentially a cyclone filter which separates heavy chars and ash particles by gravimetric method. As mentioned earlier all downstream equipment of fluidized bed reactor need to be maintained at minimum of 316 °C to prevent pipes clogging from tar condensation. Therefore, within the baghouse, there are heating electrical coil to warm up and maintain the minimum required temperature. Due to baghouse temperature limitation (400 °C), the hot gas coming out of fluidized bed reactor needs to pass through a heat exchanger before flowing through the baghouse. Moreover, cooling down hot syngas is a necessary step for downstream equipment to sample syngas composition. The gas coming out of the baghouse is normally at 4-5 psig and a temperature of 325 °C.

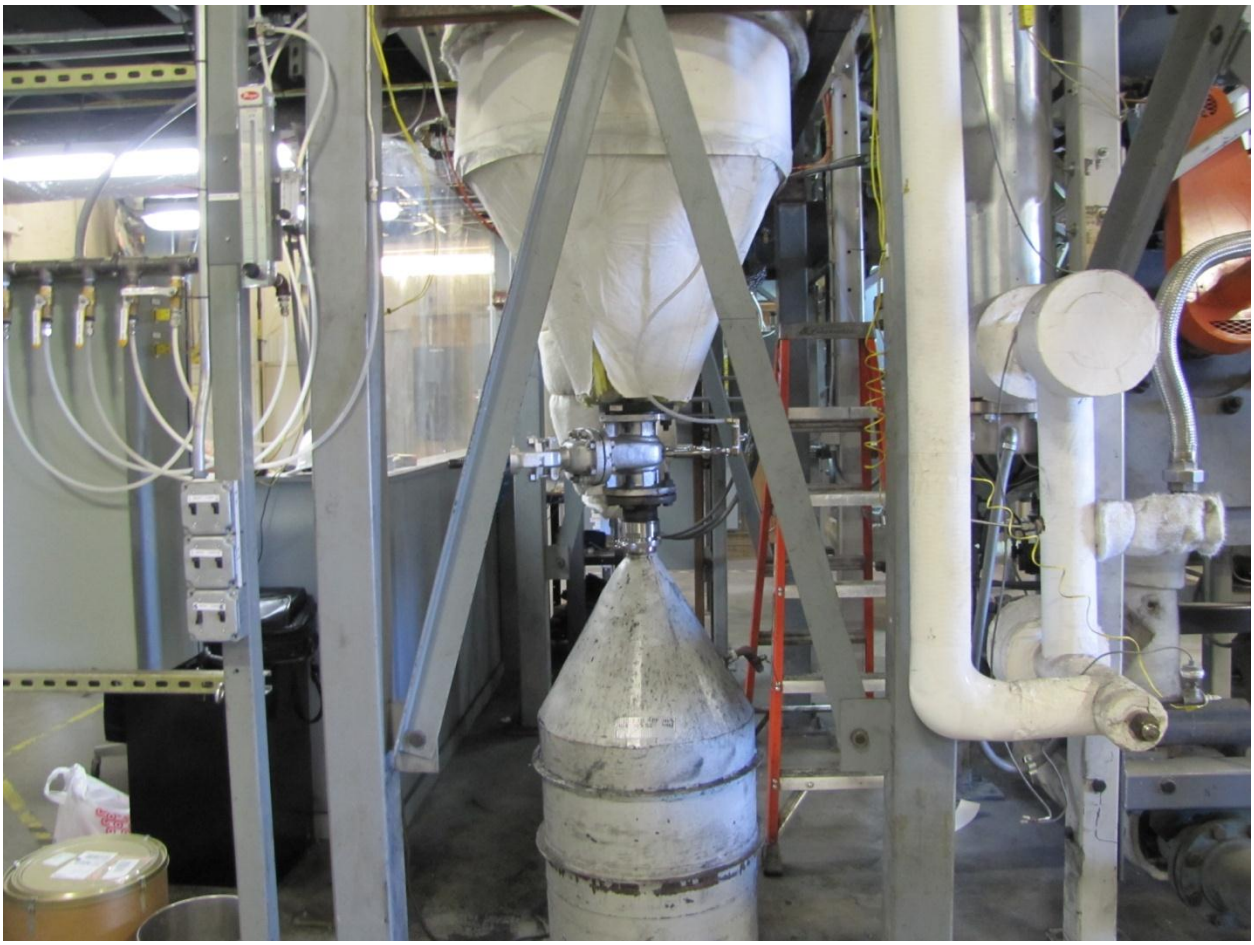

Figure 3.6: Baghouse and chars collection barrel.

3.3 – Combustion System

On the combustion side, an industrial burner made by ECLIPSE model TJ-0300 was used for producer gas combustion. The burner is rated at 879 kW and is specifically made for burning natural gas. The burner operates under the principles of non-premixed flame and staged air combustion. There are four stages within the ECLIPSE TJ-0300 burner (refer to Figure 3.7). Each of the first three stages consisted of small holes around the hollow fuel conduit. Small amount of incoming combustion air enters through these holes during the first three stages to mix

with the excess fuel to create a sub-stoichiometric combustion condition thus inhibits the formation of NO_x— due to lack of oxygen molecules to react with N_2. At the fourth stage, the remaining air and fuel will be mixed at the burner exit under lean condition so that any unburned hydrocarbons and carbon monoxides will be oxidized to form complete combustion products.

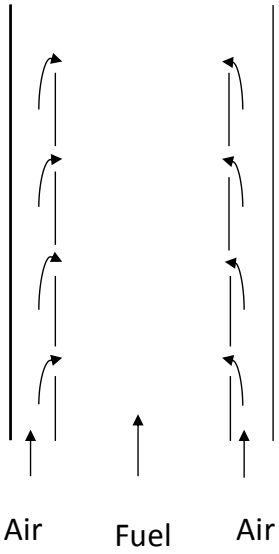

Figure 3.7: Schematic representation of ECLIPSE industrial burner.

A combustion chamber made of refractory lining is housing the burner in order to minimize heat loss (especially in the winter), prevent combustion interferences from environment (such as flame disturbance by wind or extra air is introduced which can be detrimental to NO_x emissions due to additional O_2 and N_2 that can be combined in the high combustion reaction zone), and direct the hot exhaust gas away from the testing facility. K-type thermocouples are installed at different height along combustion chamber to measure various temperatures such as exhaust flue gas temperatures and overall combustion chamber temperature. During all test conditions, the combustion chamber temperatures were always kept below 1316 °C (2400 °F) in order to protect both the combustion chamber and thermocouples. All the temperatures data, producer gas and

air flow rates are being recorded on a real-time basis into the programmable logic controller (PLC).

Figure 3.8: Combustion chamber.

Air and fuel entered the burner independently through two different ports at 90 degrees angle apart as shown in Figure 3.9. Hot syngas comes out of the baghouse at approximately 325 °C, is metered with a gas flow meter (calibrated for measuring high temperature gases) before entering burner fuel inlet.

Figure 3.9: Fuel and air inlets, air pump, and thermal gas flow meter.

Natural gas is initially used to ignite the burner and then transition to the desired flow rates of syngas begins. Depend on the test conditions, full or fraction of syngas from baghouse is flowed to the burner while the remaining unused gas directed to the flare to ensure that no harmful gases escape into the environment. It is worth to mention that only a fraction of solid chars and ash particles were able to be captured as syngas went through the cyclone filter and the flare (due to the inefficient design of cyclone filter to capture small fine particles). This ultimately hindered the calculation of fuel-bound nitrogen (FBN) balance because of the uncertainty of the exact amount of chars generated during gasification.

Atmospheric combustion air is blown to the air inlet port by an air pump. The air flow rate is measure with thermal gas mass flow meter made by Elridge Products Inc., model 8200 MPNH.

The thermal gas flow meter is inserted at location with sufficient straight run (both upstream and downstream) to allow a fully-developed laminar uniform flow profile within the conduit. Both the air pump and thermal gas flow meter can also be seen in Figure 3.9 above. The flow meter operates based on two sensors. The first sensor measures the incoming ambient temperature of the gas. The second sensor is always forced to stay at a constant temperature higher than the incoming gas stream. Therefore heat transfer from the second sensor to gas stream is directly proportional to the mass velocity of the gas stream. There isn't a need for measuring pressure within the combustion chamber since pressure change is very small in open flame combustion—pressure is assumed to be atmospheric.

3.4 – Sampling and Analysis of Syngas

In addition to gasification and combustion systems, Figure 1also illustrates sampling locations for tars, ammonia, chars, producer gas and exhaust flue gas compositions. Both syngas and flue gas compositions are measured with a micro gas chromatograph (micro GC) manufactured by Varian Inc., Model CP-4900. The micro GC is equipped with four different columns that capable of measuring CO, CO_2, H_2, N_2, O_2, CH_4, C_2H_2, C_2H_4, C_2H_6, C_3H_8 with sampling interval set at 120s.

3.4.1 – Micro Gas Chromatograph

Micro GC is a chemical analysis instrument that separate gas species in a given complex mixture sample. Micro GC consists of two phases, mobile/moving and stationary. Mobile/moving phase is an inert carrier gas such as Helium, Argon, Nitrogen and Carbon Dioxide. Stationary phase is

a layer of liquid coated on inert solid support materials that is housed by metal tubing called a column. The purpose of the columns is to separate individual gas species from a complex gas mixture. Since the stationary phase inside the column is very sensitive to water, all carrier gases need to be ultra-high purity (UHP) grade. In addition, molecular sieve/filtering system can be installed to help remove water and other impurities.

Figure 3.10 depicts the major components and working mechanism of the micro GC. The micro GC built-in internal pump draws the gas sample into the sample injector that introduces the gas onto the column head where it mixes with the inert carrier gas stream and flow through the columns. The sample gas pressure should not exceed 15 psig to prevent damage to the column head valve that would allow for continuous flow of sample gas into the columns. As sample gas progresses along the columns, various species in gas mixture will have different reaction rates with the stationary phase material, thus will be separated as they are eluding at different times, known as retention times.

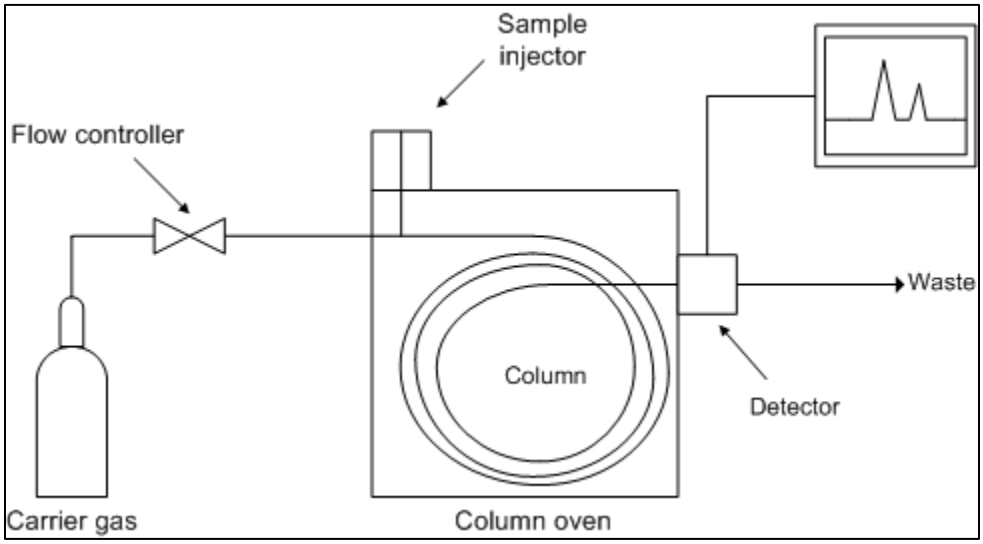

Figure 3.10: Diagram of Gas Chromatograph.
Source: Sheffield Hallam University.

The reaction rate is also a function of temperature, column dimensions, and residence time within the column—high temperature and low residence time will speed up reaction rates and would not allow enough time for gas species in the mixture to be separated when reach column exit. All operating conditions of the micro G.C. were optimized and finely tuned by Patrick Johnston of CSET research group at ISU for effectively detecting all the gas species mentioned earlier above (operating conditions can be found in Table A.2.1 of Appendix A.2). At the end of the columns, the gas will be detected and identified by thermal conductivity detector.

Before any data measurement, retention time of each interested gas species need to be determined. This was accomplished by feeding different single component gas species with helium balance gas bottles into the micro GC. Afterwards, multi-components gas bottles can be used to build calibration curves. The curves are based on first order equation with the x-axis being the volumetric concentration of gas species given by gas bottles and the y-axis represents the area under peak detected by the micro GC (in mV) with respects to gas retention time. During sampling, by correlating the known gas species retention times with detected peak areas to calibration curves, volumetric concentration of different gas species in sample gas can be found. Before and after any experiments, calibration checks were performed to make sure that the micro GC is functioned normally.

3.4.2 – NO_x Measurement

Since micro G.C. does not measure NO_x, thus two other analyzers were used to measure NO_x concentration in syngas and exhaust flue gas. The first analyzer is manufactured by Thermo-

Scientific, Model 42i Series, which operates based on chemiluminescence technology. This analyzer is only capable of measuring NO and NO_2. The second analyzer is manufactured by De Jaye Technologies. This analyzer can measures five different gas compounds—CO, HC, and CO_2 using non-dispersive infrared (NDIR) technology while NOx and O_2 using chemical cells.

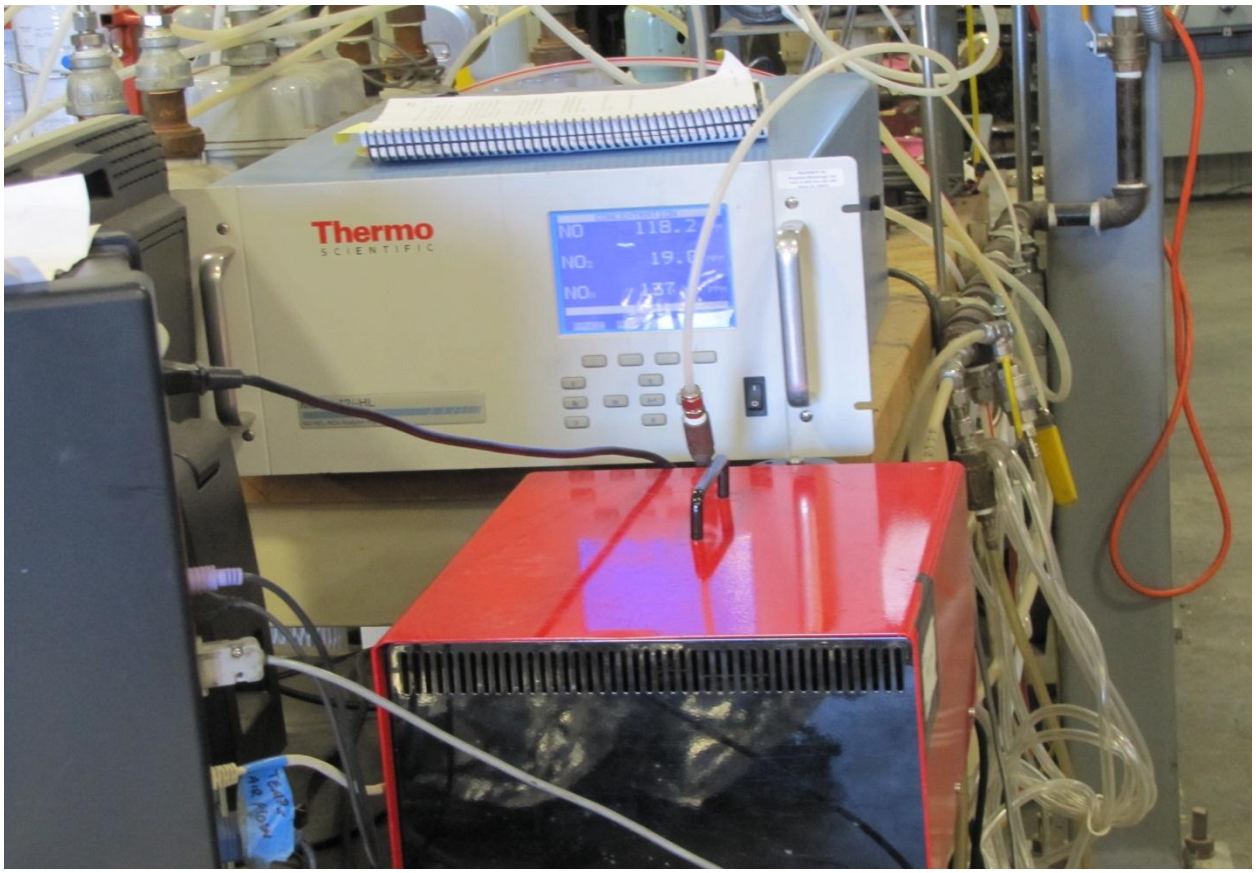

Figure 3.11: Chemiluminescence NO_x and De Jaye (in red) analyzers.

During experiments, the Thermo-Scientific NO_x analyzer is dedicated for exhaust flue gas measurements while De Jaye NO_x analyzer is used for both syngas and exhaust flue gas. This is because we wanted to validate and ensure the level of accuracy of syngas composition measured by the micro G.C. (data from micro G.C. and De Jaye analyzer are in good agreement). Moreover, the advantage of displaying real time data from De Jaye analyzer allowed us to

constantly monitor occurrence of any abnormalities within the reactor or possible leakage along the sample lines (oxygen should always read zero). Micro G.C. on the other hand, can detect more gas compounds with higher order of accuracy but its slow response time (sampling interval of 2 minutes) impeded us from actively response to abnormalities.

3.4.3 – International Energy Agency (IEA) Tar Protocol

Biomass-derived gas contains condensable and non-condensable gas as well as solid particles, therefore, appropriate method is necessary to capture and quantify gas composition. Modification of IEA (International Energy Agency) Tar Protocol was made and implemented in order to simultaneously capture ammonia, tars, and moisture in syngas. Accurate quantification of both ammonia and tars is crucial. Ammonia is the main fuel-bound nitrogen species that get convert to NO_x emissions during combustion. Tars, on the other hand, can cause technical problems such as fouling downstream equipment and hinder gas upgrade using method such as Fischer Tropsch process.

The sampling line described by the guideline consists of four modules including a module for gas preconditioning in which the sample is obtained and conditioned to a certain temperature and pressure, some sort of filter or device for particle separation and collection, the tar collection module, and the volume sampling with included temperature and pressure measurement and recording.

The IEA protocol is based on the principle of discontinuous sampling of a gas stream containing particles and tars under iso-kinetic conditions. First, sample is drawn from the syngas line after

the baghouse with a heated probe. This module is responsible for the preconditioning of the sample gas. The pressure is adjusted, and depending on the gasifier type, the gas is either heated or cooled. In the second module, all the solid components in the sample gas stream are separated from the gas and collected for further analysis. These particles consist mainly of carbon particulates known as char, but depending on the feed stock, heavy metal contents can also be found within the chars.

The third module is an impinger train with six impingers shown in 3.12. The setup aims for collecting tars and condensing water vapor out of biomass-derived gas and consists of a set of six impingers placed in temperature controlled baths (Schematic layout of impinger parts can be found in the Appendix A.2).

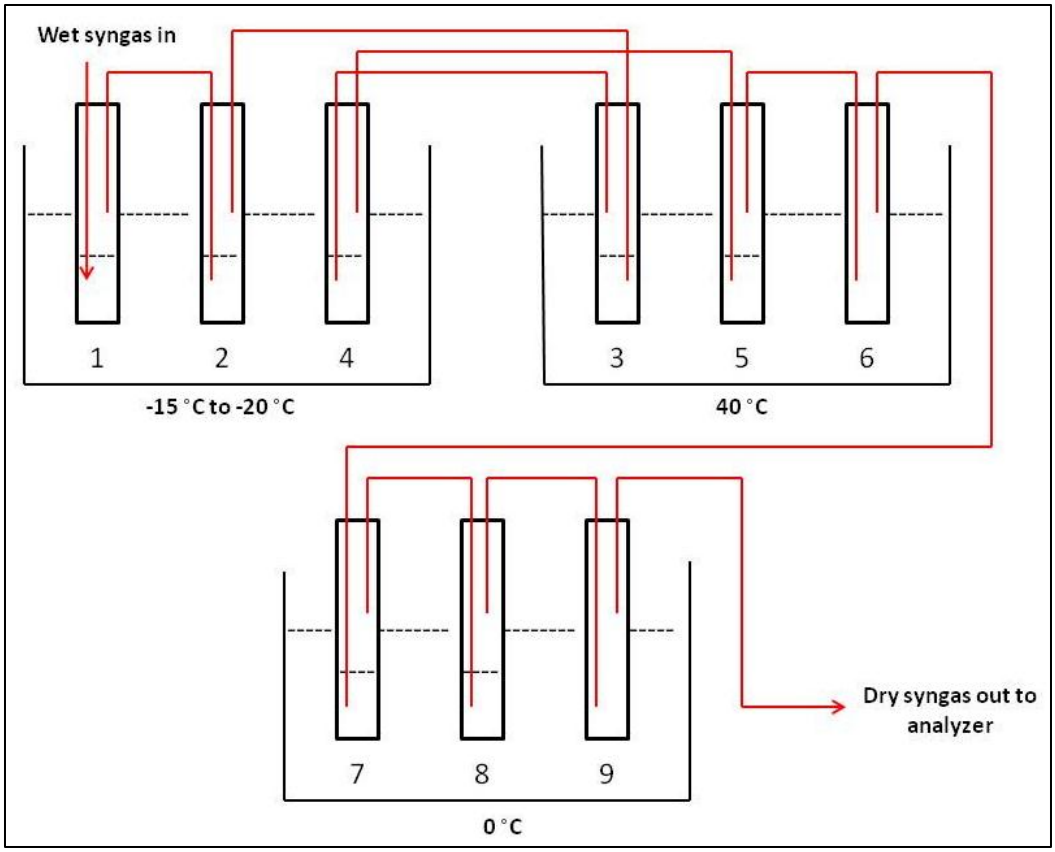

Figure 3.12: Modified IEA tar protocol impingers setup.

These impingers contained isopropyl alcohol (IPA) solvents to absorb tars. The first impinger contained 100 mL of IPA while impingers two through five filled with 50 mL, and the sixth impinger is left empty for the purpose of capturing aerosols. The impingers are placed in hot bath at 40 °C (impingers 1, 2, 4) and cold bath between -20 °C and -15 °C (impingers 3, 5, 6) using mixtures of ice, water, and salts. The low temperature of cold bath is maintained by using a mixture of water, ice and salts. A closed loop heating system was used to keep the hot bath temperature constant while the cold bath temperature was monitored and maintained manually during each test run. The hot and cold baths create two different temperature gradients that enable the hot sample gas to gradually cool down in two steps. As sample gas enters impinger one, large quantities of tars and moisture are absorbed by the vaporized IPA solvent and then

condensed (boiling point of tar is 80 °C). Subsequently, all tars and moisture will be dropped out from sample gas as they passed through the remaining impingers. Ammonia also drops out of syngas and remains within these impingers along with moisture and tars condensation as ammonia is highly soluble in water. During experiments, it was found that in addition to liquid tars and ammonium (ammonia dissolved in water) there also existed solid ammonium chloride (ammonia salts) at the bottom of impingers. Ammonia salts formation is the result of reaction of ammonia gas and hydrogen chloride gas, NH_3 (g) + HCL (g) ⟶ NH_4CL (s).

Since the IEA Tar Protocol guideline was developed for tars quantification, ammonia capturing is not very efficient therefore a second set of three impingers downstream of the first set was added to prevent ammonia slips. All three impingers are immersed in cold bath maintained at 0 °C with the first two filled with 150 mL of HPLC grade water. The amount of ammonia slip through impingers one to six depends on the amount of moisture in producer gas—the lower the moisture, the more ammonia will slip through. This is because ammonia is condensed with water thus when moisture in producer gas is low, there is not enough water for ammonia containment. In order to check if the combination of two impinger sets were able to completely capture ammonia, ammonia Drager-tubes were also used as safety measure after second impinger set. Drager-tubes are glass vials filled with chemical reagents that will react to specific chemical. The vials have pre-layers to remove other potentially interference gases so that only targeted gas is reacted with the chemical reagents. The targeted gas reacts with reagents in the tube and color changes will occur, length of color changes along the marked scale on the tubes indicates the measured concentration. Since Drager-tubes only capable of measuring small

concentration (up to 200 ppm range), it is not feasible for measuring ammonia concentration in syngas. Therefore, Drager-tubes were only used for checking ammonia slips.

Ammonia Drager-tubes were used at several time intervals during experiments and no detection was found. Dry sample gas exits second impinger set and is delivered to micro G.C. and De Jaye NOx analyzer. Volumetric flow of sample gas is measured and recorded with a calibrated dry gas meter. According to IEA Tar Protocol, minimum of seven and maximum of ten (to prevent exceeding capacity of impinger's volume) cubic feet of gas should be flown through the impinger sets effective quantification. After reaching the desired gas flow volume, the sample valve is closed and the impingers are allowed to cool down for 15 to 20 minutes to reduce the pressure within the impingers. This is very important because the sample will flows out of impingers, resulted in sample loss, if impingers are detached from sampling lines immediately after sample line is shut off.

Another precaution that needs to take into account to prevent sample loss is leakage along the all connections between every impinger. Before starting of gas sample, the impinger train sets were checked for leakage by applying pressure. After all three impinger trains are connected to syngas sampling line, the sample valve is opened for couple seconds to allow significantly small amount of syngas to flow into impinger trains. Between impinger number nine and sampling line leading to micro G.C. there existed a ball valve to allow or stop the flow to the micro G.C. This valve remained close when sample valve is opened in order to build up pressure. Next, soap-water is sprayed along impinger connections to check for possible leakages.

The sample in impingers is then transferred into separate high density polyethylene (HDPE) bottles. Samples from hot and cold baths impingers are collected into two bottles named primary and rinse. The primary bottle is used to collect samples directly out of the hot and cold bath impingers whereas the rinse bottle contained mixture of solvents and sample residues from impingers and impingers' connections. Solvents such as IPA, dichloromethane (DCM) and methanol were used to dissolve tars and water is used to collect salts within impingers and connection tubes. This is to ensure that all samples are collected. Since syngas gives off very strong odors, collection of samples from impingers needs to be taken place under a fume hood.

The HDPE bottles are tightly sealed and stored at less than 5 °C for later analysis. Sample from second set only consists of ammonia and water mixture therefore can be directly analyzed for ammonia concentration. This sample is stored in a bottle that label 7, 8, 9. Ideally, all samples should be analyze within one week to accurate quantify for ammonia because ammonia would evaporate and escape over time. All samples weight are recorded for latter calculation.

3.4.4 – Analyses of Ammonia

Since sample from hot and cold impinger sets, contain mixture of tars, water, solvents, solid ammonium chloride, and very small amount of chars escaped from baghouse, intermediate steps were required for separation of heavy tar substances from the rest.

Analyses of ammonia of collected samples from impinger set one undergo three primary steps. First, char particles in primary and rinse samples are filtered out and then going through roto-evaporating process to evaporate solvents and salts dissolved in water mixtures and retain only

tars which are quantified gravimetrically. Roto-evaporating is a similar process to distillation that allow for separation of liquid of different chemical compounds according to their boiling points. Roto-evaporating process utilizes the concept of under a vacuum condition, the substances will evaporate at a lower temperature compare to atmospheric pressure thus will not be heated by a flame. This method is more suitable compare to distillation for separation of tars from highly flammable solvents mentioned above. Moreover, the boiling point of water is 100 °C therefore if distillation process is used; tars will also evaporate along with water and solvents mixture.

The equipment is consisted of the roto-evaporating unit, chiller and a pump as shown in Figure 3.13. The roto-evaporating unit consists of six temperature treated glasses that held evenly distributed amount of samples from primary and rinse bottle. This unit is connected to both the pump and the chiller unit. The pump is used to create a vacuum condition within the unit and the chiller consists of a glass bottle to capture the evaporated samples. The temperature of the chiller is set at -105 °C in order to prevent ammonia from vaporizing and escape in gas phase. The outlet of the pump is connected to a set of three impingers (labeled 10, 11, 12) in ice bath contained HPLC grade water to collect any ammonia that might escape in gas phase.

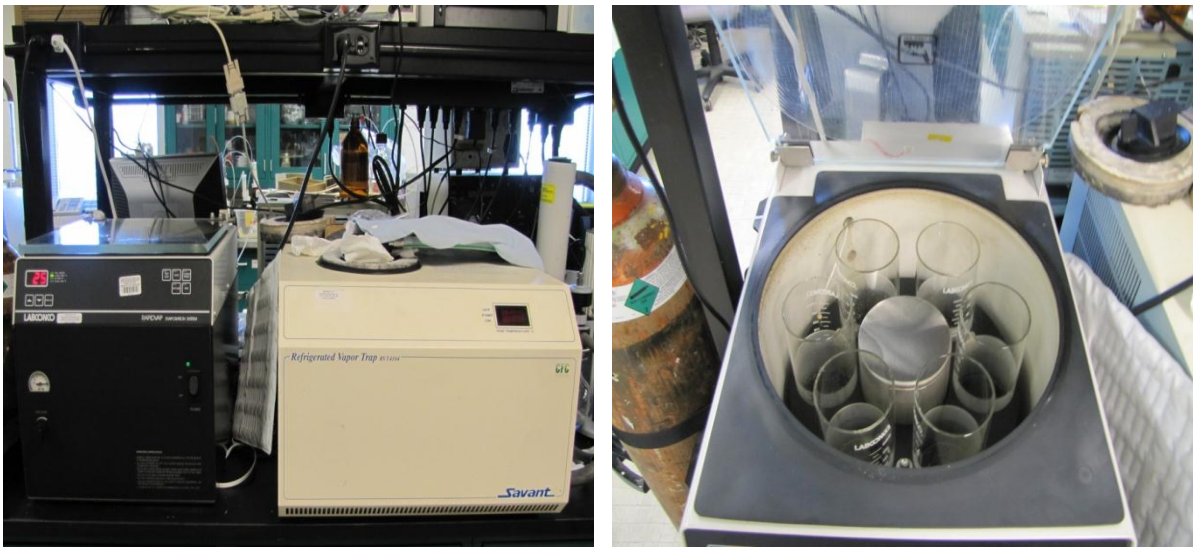

Figure 3.13: Roto-Evaporating system with chiller unit on the left (white color) and equally distributed samples on the right.

The overall roto-evaporating process took place at maximum temperature of 55 °C to prevent tars from boiling and mix with solvents and salt-water. The six sample glasses are subjected to revolving motion throughout evaporating process so that uniform temperature can be achieved. The process can take up to between 4 to 8 hours depend on how much water was used when rinsed out the syngas residues from impingers and impinger's connection tubes. If unavoidable large amount of water was used to clean out syngas residues then a separation flask as shown in Figure 3.14 can be used to remove water from sample before pouring into roto-evaporating glasses. Moreover, the roto-evaporating process can also be speed up by adding methanol. After the process is completed, indicates by only dry tars on the bottom of the glasses, the sample collected from chiller is poured into another HDPE bottle labeled "Distillated." The weights of all six glasses before and after the process are recorded for tar quantifying concentration.

Figure 3.14: Water-sample separation in aiding roto-vap process.

The second step involves using Aquanal ammonium test kits containing three reagents to shift the pH value of the roto-vap solution to convert free ammonia in sample to ammonium ions. Ammonium ions are then reacted with hypochlorite and thymol to cause color change of solution (green). Intensity of green color is directly proportional to ammonia concentration in the sample.

The third step is to pass the color changed solution to an Ultraviolet-visible spectrophotometer (UV-Vis). The UV-Vis measures the energy of light before entering and after leaving the sample. The difference is the amount of absorbed energy and is directly proportional to the ammonia concentration in the sample. Ammonia concentration in syngas is then calculated by using the known ammonia concentration in analyzed samples and the measured gas volume flow during sampling time interval.

3.4.5 – Determining Water Content in Syngas

Biomass-derived gas from gasification process contains certain amount of water vapor which heavily depends on feedstocks and operation conditions. Determining water content in syngas is very important since it directly affect gas heating value, laminar flame speed and flammability limit. Typically, biomass-derived gas from air-blown fluidized bed gasifiers ranges from 13 to 20 wt% (Hasler and Nussbaumer, 1999).

Karl Fischer Titration method was used to determine water content from collected sample in impingers. This method determines water content in substances by measuring the electricity needs for electrolysis process to produce iodine amount to completely react with water in substances. Right before roto-evaporating process, small quantity (around 1 mL) from primary sample after filtered is saved for water tests—only the primary sample was used for it not being diluted by solvents. The Titrator measured amount of water in the sample on mass basis—percent of water in the sample. Thus longer gas sampling time interval (higher total gas volume flow) would give higher water reading. Therefore, measured water from sample needed to be correlated to water content within syngas by using the measured volume of dry gas flows during recorded sampling time interval. Assuming ideal gas condition, the mass flow of dry syngas can be computed with measured temperature and pressure. $R_{dry\ gas}$ is found by dividing the universal gas constant $\bar{R}$ by dry gas molecular weight which is determined from dry gas composition measured by micro G.C. Finally, actual mass percentage of water in syngas is found by dividing mass of water collected in primary (wt% from Titrator times mass of primary sample) by sum of dry gas, ammonia (determined from UV-Vis), and water mass in primary sample. This water content is then used to convert dry gas composition measured by micro G.C. into wet gas basis—

the actual syngas composition necessary for determining amount of air needs at different combustion equivalence ratios.

Calibration curve is built using different mixtures of isopropanol and water with specific concentrations of water content closes to the range expected of the samples. The deviation of measured value from actual value is taken into account for the correction of the final calculation of water content from actual sample. For every sample, three water tests were run and then took the average. The calibration curve can be found in the Appendix.

3.5 – Sampling of Exhaust Flue Gas

For exhaust flue gas sampling, sampling line is connected through the combustion chamber at approximate distance of 4 meters above the flame height. The flue gas is then passed through a set of three impingers sitting in cold bath at 0 °C for condensing out the water in the flue gas stream.

Figure 3.15: Water condensing impingers set for exhaust gas.

The first two impingers are filled with 150 mL of HPLC grade water and the last one is empty to capture and minimize the amount of solid particles remain in the gas. The distance from flue gas sampling line to analytical workstation is about 20 meters therefore a vacuum pump is used to pull the flue gas sample to micro G.C. and two NO_x analyzers. A particulate filter is installed before the vacuum pump to prevent particulate matters from entering and damaging analytical equipments. A pressure gage and rotameter are placed downstream of the pump to measure the pressure and control flue gas flow rates. All analytical equipments are calibrated before and after each experiment with calibration gases to make sure they are correctly functioned.

Chapter 4 – Results and Discussion

4.1 – Feedstock

Three types of biomass feedstock were used in this study—pine, oak mix with maple, and seed corn. Pine wood and oak combine with maple wood were in pellets form. The pellets have dimensions of 0.25 inches and 0.5 inches for diameter and length respectively. The biomass feedstock for this study were chosen on the basis of wide availability and have high potential for sustainable supplies which is essential for cost reduction due to the economics of scale and smaller feed storage. In addition to the variation in overall composition, all feedstock have considerable different nitrogen contents. This correlates well to our purpose of study on the effects of enriched-air and steam blown gasification on syngas composition and formation and destruction of ammonia. The ultimate and proximate analyses of the biomass feedstock used in this study are shown in Table 4.1. The analyses were performed by Huffman Laboratories Inc. Notice that the analyses only include main species (CHNOS) but not trace species such as chloride and minerals.

Table 4.1: Proximate and Ultimate Analysis of Different Biomass Feedstock.

Feedstock	Wood (Pine)	Wood (Maple + Oak)	Seed Corn
	Proximate Analysis (Wt%)		
Volatiles	74	75.11	66.43
Fixed Carbon	16.66	16.81	17.15
Moisture	8.9	6.25	15.01
Ash	0.43	1.83	1.4
	Ultimate Analysis (Wt%)		
C	47.52	46.56	40.07
H	6.5	6.24	7.1
N	0.05	0.14	1.4
O	46.36	46.13	50.5
S	0.01	0.02	0.17

The accuracy of the above results is as follow:

- Carbon and Hydrogen (C-H): ± 0.3% absolute
- Nitrogen (N): ± 0.2% absolute
- Sulfur (S): ± 0.05%T absolute
- Oxygen (O): ± 0.5% absolute
- Volatiles and fixed carbon: ± 1.0% absolute
- Moisture: ± 0.1% absolute
- Ash: ± 0.1% absolute

The term absolute means that the results can be reproduced within the indicated plus/minus ranges.

4.2 – Test Conditions

Tests were conducted for three different biomass feedstock with each feedstock at three different oxygen concentrations in the gasifying agent. Therefore, nine different set of syngas composition were obtained. For each set of syngas, the burner was operated at various fuel flow

rates and equivalence ratios. The equivalence ratio (ER) is defined as the ratio of actual air-fuel ratio to the stoichiometric air-fuel ratio. All combustion test conditions were chosen in the lean mixture ranges to ensure the maximum temperature within combustion chamber below 2400 °F. This temperature is set by the burner manufacturer as safety measure for not damaging the combustion chamber and the burner itself. The whole combustion system will automatically shut down once the safety temperature is reached. The complete test matrix is shown in Table 4.2. Notice that only two fuel flow rates were tested for all oxygen enriched-air and steam cases compared to three fuel flow rates for all air gasification cases. This is due to limited testing time and available feedstock. Moreover, we expect that NO_X emissions will increase as fuel flow rates increase for both air and oxygen enriched-air and steam gasification.

Table 4.2: Operating Conditions.

FeedStocks	Nitrogen Content (wt%)	Gasifier Condition	Burner Fuel Flow Rates, pounds per hour (pph)	Burner Equivalent Ratio
Seed Corn	**1.4**	Air Blown	100, 150, 250	1.12-2.34
		30% O_2 Enriched, Wet v/v%	100, 250	1.09-2.10
		40% O_2 Enriched, Wet v/v%	100, 250	1.07-2.10
Pine Wood	**0.14**	Air Blown	100, 150, 250	1.09-1.72
		30% O_2 Enriched, Wet v/v%	100, 250	1.18-2.04
		40% O_2 Enriched, Wet v/v%	100, 250	1.16-1.96
Maple + Oak Wood	**0.05**	Air Blown	100, 150, 250	1.2-3.0
		30% O_2 Enriched, Wet v/v%	100, 250	1.24-1.68
		40% O_2 Enriched, Wet v/v%	100, 250	1.17-2.22

4.3 – Syngas Composition

Table 4.3 summarized ammonia concentration, gas composition (wet basis), lower heating value (LHV), and adiabatic flame temperature of the syngas derived from each feedstock at different oxygen enriched- air condition. Lower heating value and adiabatic flame temperatures are calculated using Engineering Equations Solvers, EES. Adiabatic flame temperatures are evaluated at stoichiometric condition with only H_2O, CO_2, and N_2 as products. As Table 4.3 indicates, all the main gas constituents have the same increasing trends for all biomass feedstock when oxygen percentage increases from 21 to 40 vol. %. Therefore, only results using one feedstock will be chosen for discussion (pine wood) but the comparison of gas amounts among biomass feedstock will also be included.

The syngas composition (except ammonia and tars) was measured using a micro G.C., which indicated a steady reading throughout the measurement. For each feedstock, two tests were run and the results showed in Table 4.3 are taken as the average with maximum error of ±2%.

Table 4.3: Syngas Composition Using Different Biomass Feedstock at Different Oxygen-Enriched Air Concentration (% Volumetric Wet Basis).

Feedstock	Pine Wood			Maple + Oak Wood			Seed Corn		
Oxygen Percentage	21% O_2 (% v/v)	30% O_2 (%v/v)	40% O_2 (%v/v)	21% O_2 (% v/v)	30% O_2 (%v/v)	40% O_2 (%v/v)	21% O_2 (% v/v)	30% O_2 (%v/v)	40% O_2 (%v/v)
H_2	9.47	14.92	16.09	11.33	15.04	16.65	4.43	5.46	5.86
CO	16.09	19.23	21.50	16.91	18.40	19.93	12.42	13.09	13.49
CO_2	13.09	18.03	19.51	13.56	17.92	19.68	10.91	12.17	12.74
N_2	38.03	15.06	5.76	39.02	17.80	5.20	41.60	15.36	5.02
NH_3	0.016	0.02	0.0157	0.06	0.09	0.11	0.53	0.68	0.89
NO_X	0.01	0.022	0.027	X	X	X	0.03	0.045	0.041
H_2O	13.05	24.35	29.75	9.97	21.94	27.34	21.65	44.56	55.85
CH_4	5.5	6.29	7.1	5.27	6.38	6.82	3.59	4.14	4.24
C_2H_2	0.091	0.10	0.12	0.07	0.083	0.097	0.16	0.15	0.14
C_2H_4	1.56	1.67	1.99	1.18	1.48	1.70	1.76	1.88	1.97
C_2H_6	0.39	0.38	0.46	0.26	0.43	0.42	0.27	0.31	0.32
C_3H_8	0.209	0.206	0.30	0.07	0.195	0.17	0.204	0.265	0.24
Tars (g/m^3)	13.78	18.67	19.55	X	8.18	6.62	13.47	X	11.39
LHV (MJ/kg)	5.77	7.27	8.26	5.58	7.11	8.09	4.28	5.22	5.49
T_{ad} (K)	1929	2006	2050	1932	1999	2042	1744	1765	1755

4.3.1 – Hydrogen Content

The hydrogen content in syngas for pine wood ranges between 9.5 to 16.1 vol. % which equates to approximately 70% improvement. The H_2 content increases as oxygen percentage increases from 21 to 40 vol. %. Since the fluidized bed temperature was kept constant, additional steam was introduced as oxygen percentage in air increased. The steam to oxygen ratio (S/O, where oxygen is the sum of pure oxygen and percentage of oxygen from air) for 30 and 40 vol.% are 1.24 and 1.32 respectively. This increase in steam is the main contributing factor for the increase of H_2 concentration in syngas. The increase in oxygen percentage would be more likely to have adverse effects on hydrogen concentration because more hydrogen is burnt. The introduction of steam into reactor favors the water-gas reaction, water-gas shift reaction, and steam reforming reaction indicated by equations 2.6 to 2.8 respectively.

According to Kumar et al. (2009) and Lv et al. (2004), reactions associated with equations 2.6 to 2.8 are most favorable when gasification temperature is above 800 °C where high temperature provides energy for the endothermic reaction of steam to produce hydrogen. This is evidenced from the high water content in syngas composition provided in Table 4.3. The boosted water from 13 to 29 vol. % indicates that a large fraction of steam does not react with syngas to increase hydrogen content at a fixed bed temperature of 800 °C. Ultimate analyses of feedstock from Table 4.1 show that seed corn has the highest hydrogen content followed by maple/oak and pine wood. Thus, one would expect that hydrogen content in syngas would be highest for seed corn; however, our data indicate that seed corn has the lowest hydrogen content. One possible explanation is that since seed corn has almost double the moisture content compared to pine and maple/oak wood, more energy from the oxidation reaction is utilized during the drying stage.

Thus, less energy is left for combustion reaction to drive the endothermic reactions of steam for H_2 and CO production. The H_2 and CO contents in syngas for seed corn are only improved by 6.7% and 8.7%, respectively, which are relatively low when compared to those of the other two feedstocks.

4.3.2 – CO Content

Similar to H_2, carbon monoxide increases when oxygen percentage changes from 21 to 40 vol. %. However, the magnitude of the increase in CO is much less than H_2. CO ranges from 16.1 to 21.5%, 16.9 to 19.9%, and 12.4 to 13.5% for pine wood, maple/oak wood, and seed corn, respectively. When more oxygen is introduced into the reactor, carbon conversion efficiency is increased because extra oxygen is available to enhance the combustion reactions, therefore releasing more heat to accelerate gasification process. Most gasification processes do not reach true equilibrium (due to the short residence time). Therefore by accelerating the gasification process, there is a chance to further crack down large amount of carbons within chars. Oxygen, steam, and carbon dioxide are all possible candidates for reacting with chars to produce CO_2, CO, and CH_4 as shown by equations 4.1 to 4.3

$$\text{Char} + O_2 \longrightarrow CO_2 \text{ and } CO \quad (4.1)$$

$$\text{Char} + CO_2 \longrightarrow CO \quad (4.2)$$

$$\text{Char} + H_2O \longrightarrow CH_4 \quad (4.3)$$

In addition, an increase in CO could be a result from increasing steam-carbon ratio (carbon is the carbon fraction in the fuel). Higher S/C ratio favors water-gas reaction in Eq. (2.6). The S/C for

pine wood for 30 and 40 vol. % are 0.235 and 0.237 (mol/mol), respectively. Again a marginal increase in CO content shows that excess steam simply leaves the gasifier unreacted.

4.3.3 – CO_2 Content

The CO_2 amounts in syngas for both woods are between 13 and 20 vol. %, and between 11 to 13 % vol. for seed corn. Notice that when oxygen percentage increases to 30 and 40 vol.%, the difference between CO and CO_2 becomes smaller. The increases in CO_2 are expected because higher amount of O_2enhances CO conversion to CO_2. Moreover, the presence of steam helps increase the H_2 amount but at the expense of oxidizing CO to CO_2. Since the amount of CO_2 does not increase in the same magnitude as the oxygen fed, this indicates that some of CO_2 react with chars thus limiting the final CO_2 output.

4.3.4 – Light Hydrocarbons Content

For all three biomass feedstock, very little increase in CH_4 and light hydrocarbons is observed. Pine wood has the highest increase at 1.58 vol. %, followed by Maple/Oak at 1.55 vol. %, and seed corn at 0.65 vol. % when oxygen percentage is increased from 21 to 40%. All C_2's are well under 0.5% except for ethylene (C_2H_4) which is between 1.2 and 2.0 vol. %. An improvement in CH_4 yield is achieved through Methananation reactions due to more CO, H_2 and CO_2 as discussed earlier. Methanantion reactions are given by equations 2.8 to 2.10.

4.3.5 – Gas Heating Value

Syngas heating value is directly proportional to the concentration of combustible gas constituents such as H_2, CO and CH_4 and is inversely proportional to water and nitrogen concentration. As oxygen percentage increases from 21 to 40 vol. %, combustible gas increases and nitrogen decreases, thus resulting in higher gas heating value. Results show that the lower heating values have increased up to 28% and 43% for seed corn and woods, respectively. The small improvement in seed corn LHV is due to substantial increase of moisture in syngas, from 22 to 56 percents.

4.3.6 –Ammonia and NO_X

It has been shown that ammonia is the dominant N-containing species during biomass gasification and its concentration in syngas increases as nitrogen content in feedstock increases (Zhou et al., 2000). Additional ammonia formation can result from interaction between steam and char-N (Tian et al., 2007). The presence of steam generates significant amount of hydrogen radicals which can react with radicals in solid char that enhance the breakdown and gradual hydrogenation of char-N into NH_3 (Yu et al., 2007). Thus ammonia concentration increases as oxygen percentage increases due to additional steam input to keep bed temperature fixed at 800 °C. Among the three feedstock studied, maple/oak wood has the most significant increase in ammonia concentration, a 77% increase from air to 40 vol. % oxygen enrichment whereas seed corn only increase by 68%. Pine wood on the other hand, shows an increase in ammonia concentration from 21 to 30 oxygen vol. % and then decreased at 40 vol. % oxygen. As Table 4.3 indicates, pine wood has the largest hydrogen increment from 21 to 40 vol. % oxygen. Therefore there is a high possibility that the reaction between hydrogen radicals to form di-

molecular hydrogen is stronger compared to hydrogen radicals reaction with N-containing species to form ammonia. Furthermore, pine wood has the lowest nitrogen content but its N_2 concentration at 40 vol% oxygen is the highest, indicating that more feedstock-bound nitrogen is converted to di-molecular nitrogen rather than reacting with hydrogen radicals to form ammonia. Another rationale for the decrease of ammonia concentration is through the simultaneous destruction of ammonia in the presence of oxygen:

$$4NH_3 + 3O_2 \rightarrow 2N_2 + 6H_2O \quad (4.4)$$

$$4NH_3 + 5O_2 \leftrightarrow NO + 6H_2O \quad (4.5)$$

The above two reactions can explain the decrease in ammonia and increase in N_2, H_2O, and NO_X as oxygen percentage rises. For seed corn, an inverse trend of ammonia and NO_X compare to pine wood is observed. The NO_X level increases as ammonia concentration increases. This is explained by the inhibition of ammonia destruction in the presence of high steam concentration. McKenzie et al. (2007) reported that the destruction of ammonia in the presence of 2000 ppm oxygen is 19%, however, when both steam and oxygen are used (15% H_2O + 2000 ppm O_2) only 4% of ammonia is destroyed. The water content in seed corn syngas is much higher compared to pine wood, thus having a greater effect on inhibition of ammonia destruction. Notice that the drop in NO_X level from 30 to 40 vol. % oxygen for seed corn is not an indication of the decrease in concentration but due to the relative small increase in NO_X percentage compared to water. Thus, NO_X appears to be decreasing when the gas is corrected from dry to wet concentration.

NO_X values were measured only for pine wood and seed corn. This is because there were technical difficulties with the NO_X analyzer used during experiments and a solution was not

found during the allowable experiment time frame. Additionally, re-tests were not an option because maple/oak wood feedstock were running low and the local supplier for this wood ran out of business.

4.4 – NO_x Emissions from Syngas Combustion

NO_X emissions resulting from syngas combustion are corrected to 3% oxygen level in the exhaust gas using the following equation:

$$NO_X\ @\ 3\%\ O_2 = \ NO_x\ raw\ data * \frac{(1-0.03)}{\left(1-\frac{\%\ O_2}{100}\right)} \tag{4.6}$$

The above formula is a common practice used in industry to characterize burner emission performance. The purpose of correcting to 3% O_2 level is to remove the dilution effect so that fair comparisons of emission levels can be made. Because oxygen and NO_X are measured and quantified at the same points therefore if the mass of the emitted NO_X remains the same, then increasing air supply can lead to reduction of NO_X in mole fraction or ppm. Equation 4.6 will give higher NO_X values compare to raw data when O_2 percentage in exhaust is greater than 3% (i.e., more air dilution) and lower values when O_2 is lower than 3%. The equivalent ratio (ER) used on the burner side is defined the same as in gasification—ER greater than 1.0 indicates lean combustion.

4.4.1 – Emissions Using Maple and Oak Wood

Figures 4.1 to 4.3 show NO_X emissions from combustion of syngas resulting from air blown to 40% oxygen enriched air-steam mixture gasification. In Figure 4.1, three different fueling were tested, i.e. 100, 150, and 250 pounds per hour (PPH), corresponding to different heat rates (70.3, 105.4, and 175.7 kW). Different fueling rates were used for different feedstock and syngas conditions to ensure the successful operating of the burner.

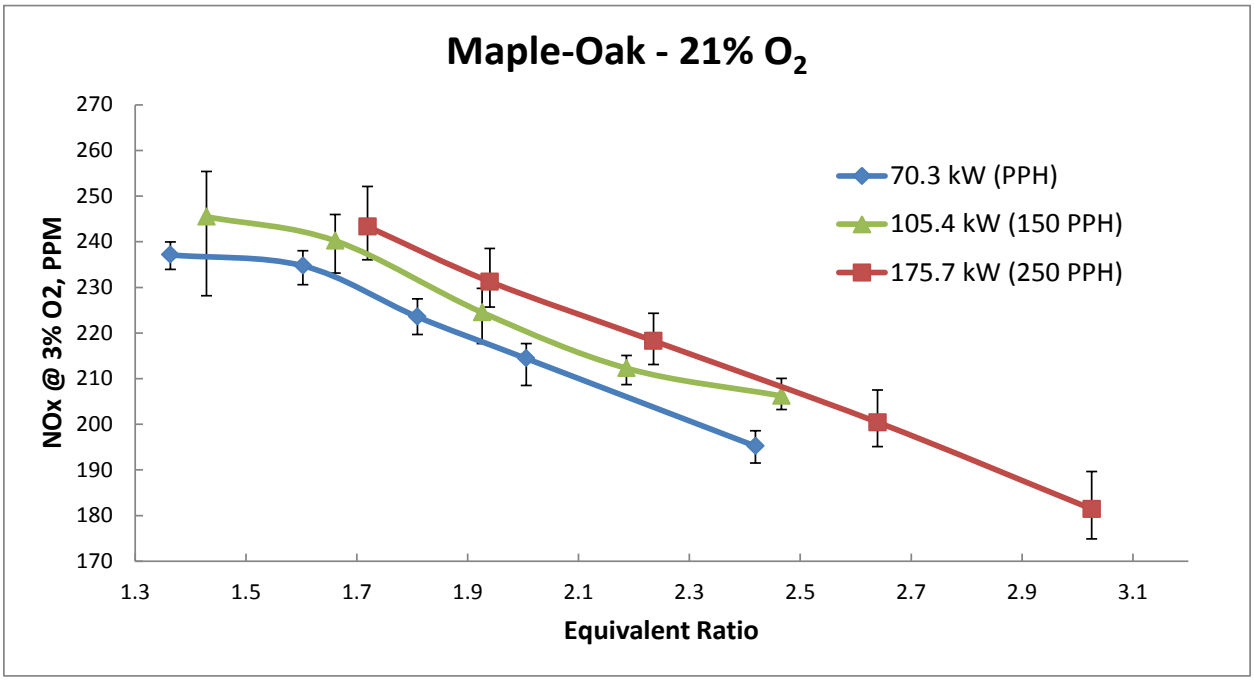

Figure 4.1: NO_X emissions using maple/oak wood resulting from air blown gasification at 100/150/250 PPH.

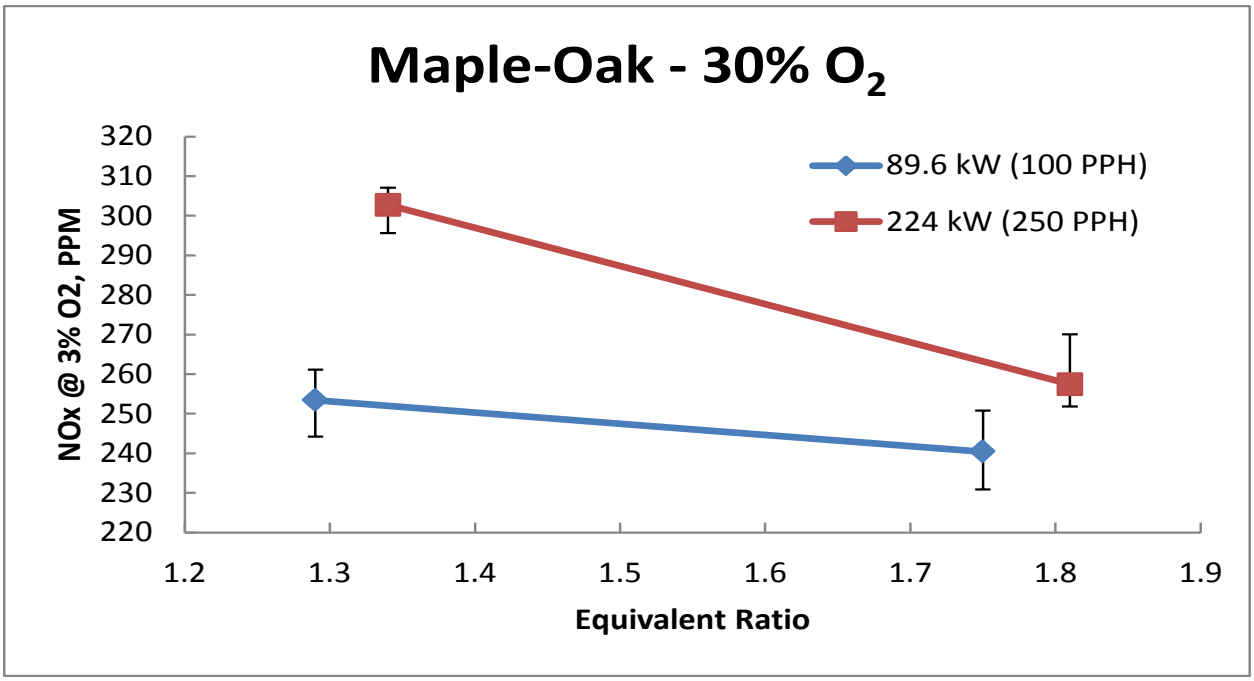

Figure 4.2: NO_X emissions using maple/oak wood resulting from 30% oxygen enriched air-steam mixture gasification at 100/250 PPH.

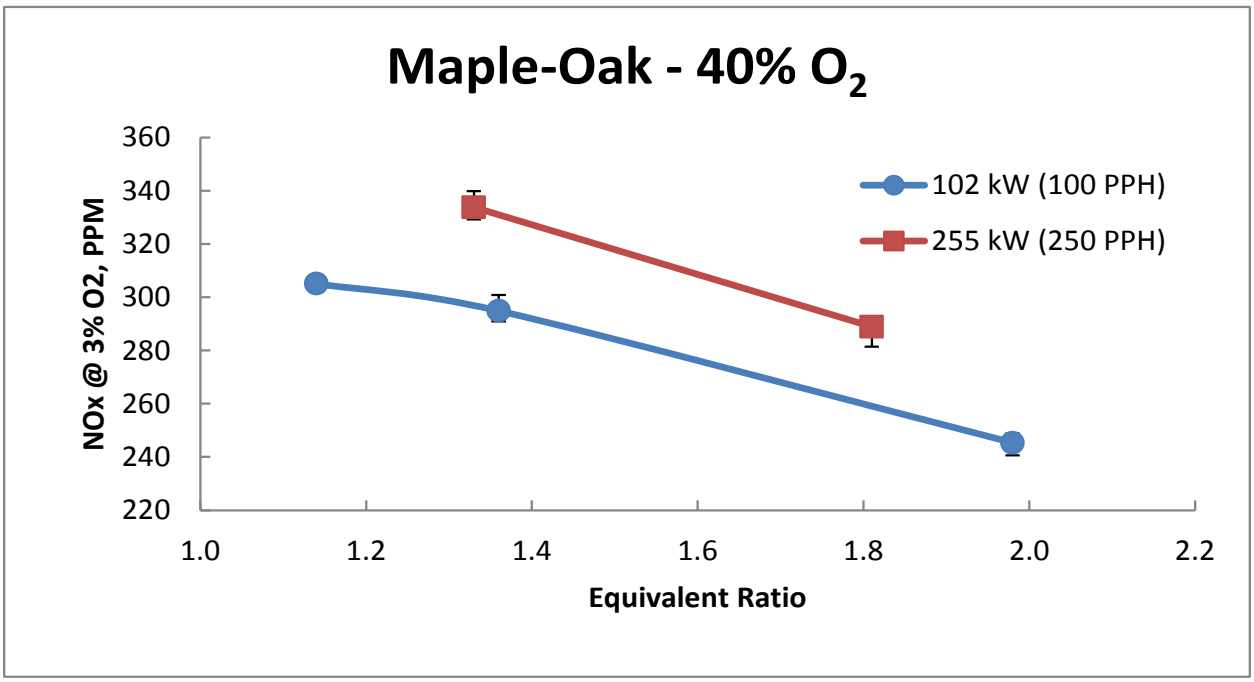

Figure 4.3: NO_X emissions using maple/oak wood resulting from 40% oxygen enriched air-steam mixture gasification at 100/250 PPH.

As expected, NO_X emissions decrease with increasing ER (i.e., leaner conditions) and increase as fuel flow rates increase. The decrease of NO_X emissions as ER increases is attributed to lower combustion temperature at leaner conditions which is not favorable for thermal NO_X formation. The heat rates increase with increasing fuel flow rates which cause the combustion chamber and exhaust gas temperature to rise, thus enabling the breaking of N_2 to react with available oxygen or OH radicals to form NO_X and eventually contributing to the overall increase of NO_X emissions. Additionally, the increase in fueling rate also results in a large flame zone (combustion region) where more NO_X is formed.

It is well-known that NO_X formation is mainly a function of thermal NO_X, fuel-NO_X, and prompt NO_X, of which thermal and fuel NO_x are generally more significant compared to prompt NO_X. Table 4.3 depicts that ammonia concentration and heating value of syngas increase from air blown to oxygen enriched air-steam mixture gasification. The increases in ammonia and heating value of syngas correlate well with the higher overall NO_X emissions illustrated in Figures 4.4 and 4.5—higher ammonia and heating value simultaneously contribution to fuel and thermal NO_X.

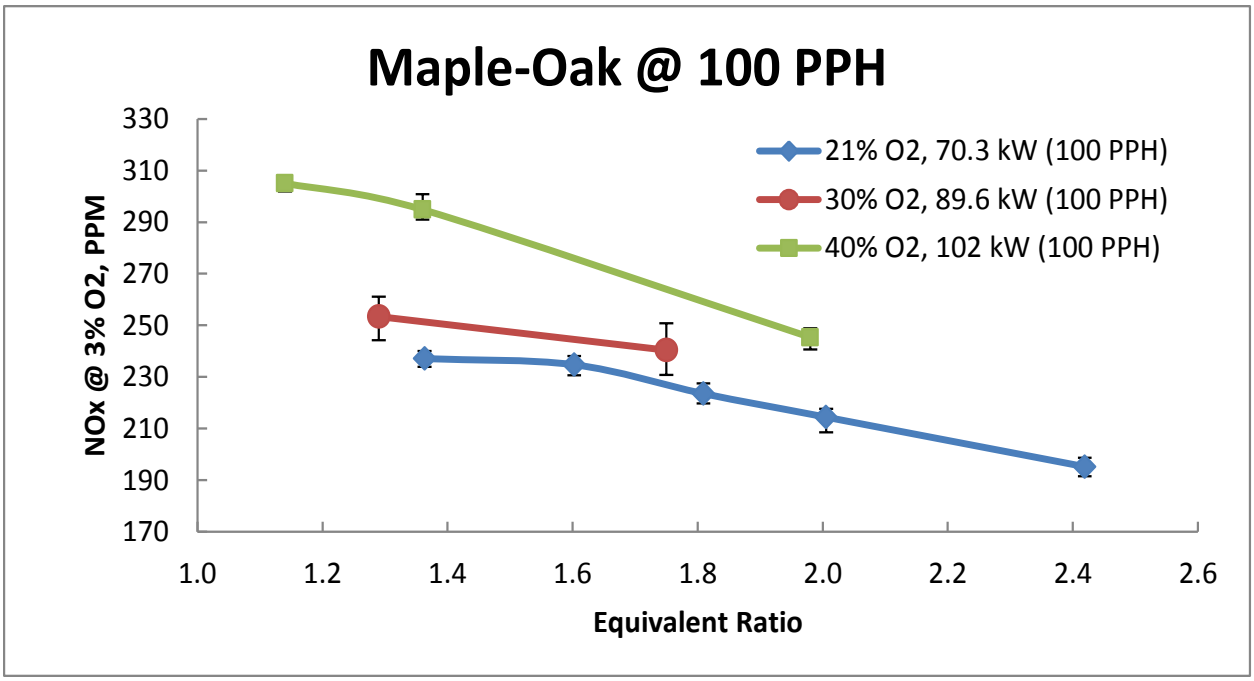

Figure 4.4: NO_X emissions comparison between air blown and oxygen enriched air-steam mixture gasification using maple/oak wood at 100 PPH.

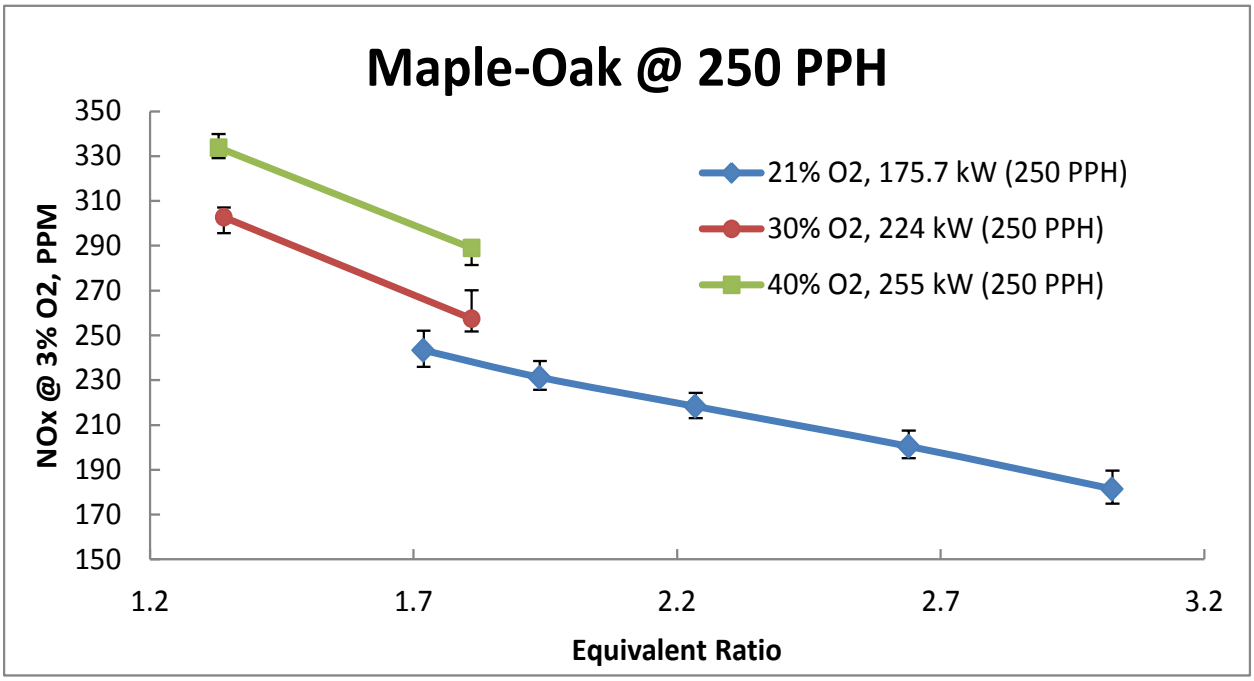

Figure 4.5: NO_X emissions comparison between air blown and oxygen enriched air-steam mixture gasification using maple/oak wood at 250 PPH.

There is a noticeably higher increase in NO_X emissions for 40% O_2 than 30% O_2 in comparison to syngas from air blown gasification. NO_X emissions only increase approximately 30 to 70 ppm when comparing syngas combustion from air blown to 30% O_2 enrichment gasification whereas NO_X emissions from 40% O_2 enrichment case is in the range of 80 to 150 ppm higher than air blown gasification case. The significant increase in NO_X for 40% O_2 enrichment is from both thermal and fuel NO_X. Syngas from the 40% O_2 case has higher adiabatic flame temperature than syngas from the 30% O_2 case. Ammonia concentration increases by 0.029% from air blown to 30% O_2 case and increases by 0.017% from 30% O_2 to 40% O_2 case. Hence one expects that overall NO_X emissions attributed to fuel-NO_X will increase. The adiabatic flame temperatures of syngas is 1932, 1999, and 2040 K for air blown, 30% O_2, and 40% O_2 case, respectively. Notice that thermal NO_X increases exponentially when temperature is above 1600 K (Baukal, 2001) therefore thermal NO_X for 40% O_2 case is more significant than 30% O_2 case.

4.4.2 – Emissions Using Pine Wood

Figures 4.6 to 4.8 show the NO_X emissions using pine wood resulting from air blown to 40% O_2 enrichment gasification.

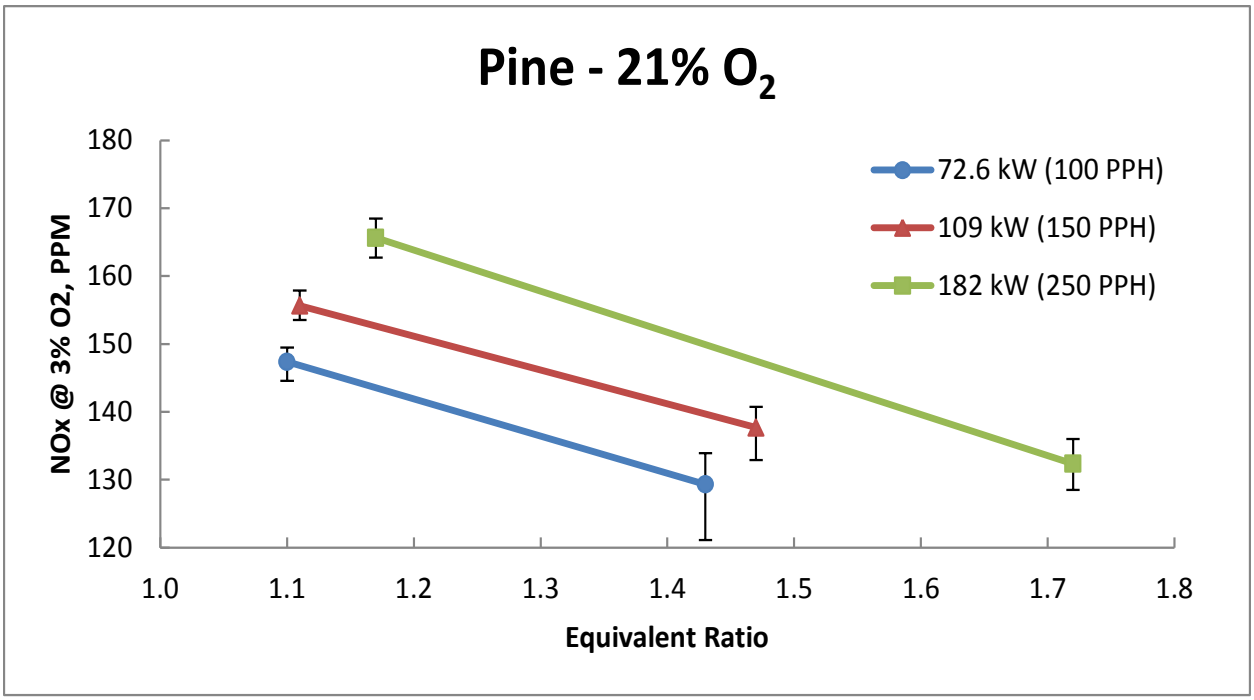

Figure 4.6: NO_X emissions using pine wood resulting from 21% air blown gasification at 100/150/250 PPH.

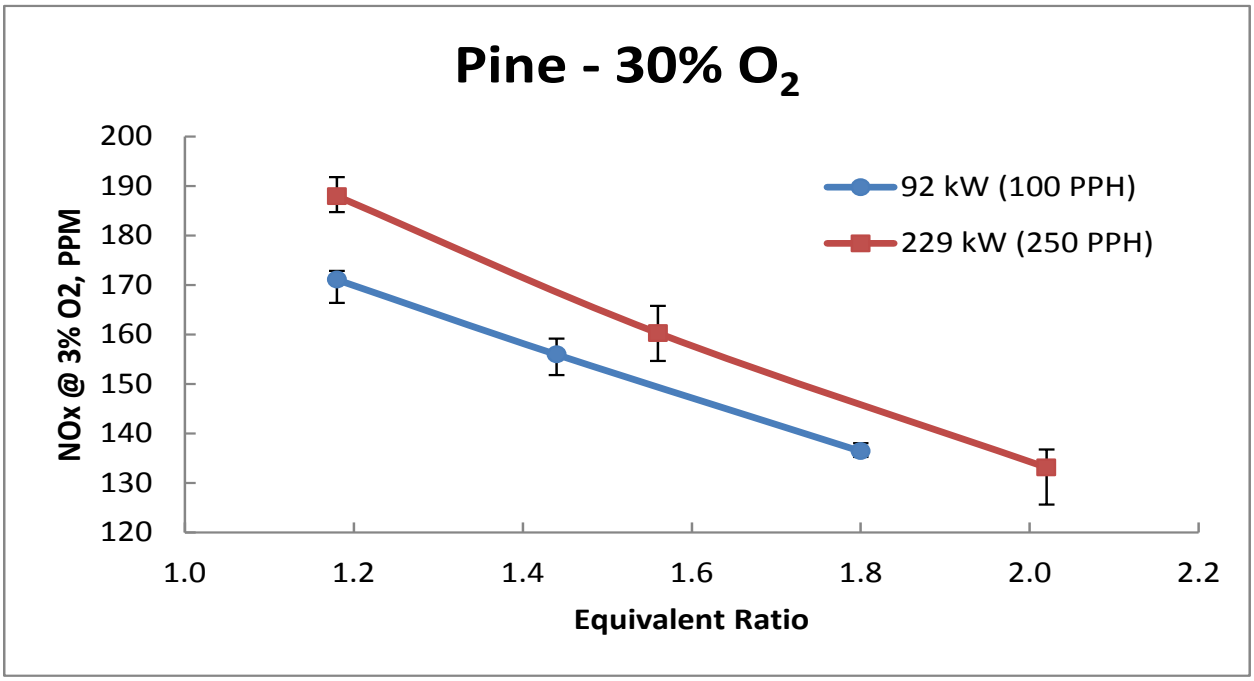

Figure 4.7: NO_X emissions using pine wood resulting from 30% oxygen enriched air-steam mixture gasification at 100/250 PPH.

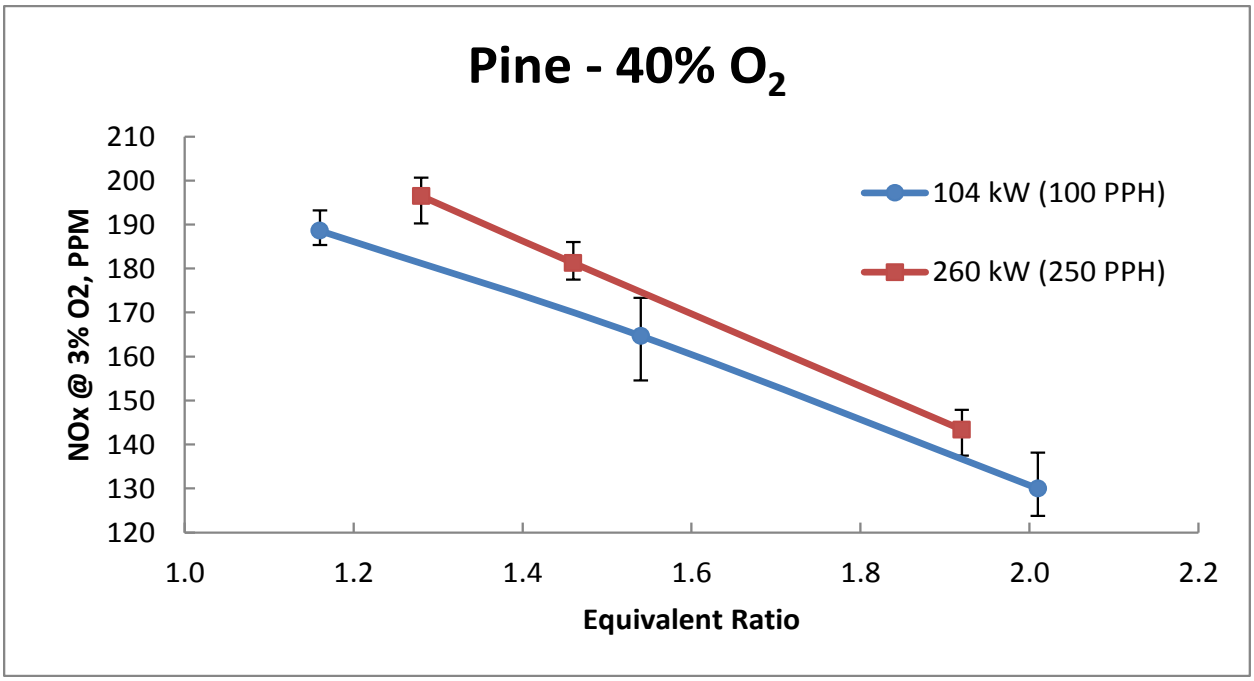

Figure 4.8: NO_X emissions using pine wood resulting from 40% oxygen enriched air-steam mixture gasification at 100/250 PPH.

The emissions exhibit similar trends to those in the maple/oak wood case, i.e., monotonic decrease in NO_X emissions with leaner combustion and lower fuel flow rates. However, NO_X emissions resulting from syngas combustion at all gasification conditions are in the order of 80 to 150 ppm lower in comparison to the maple/oak wood cases. As shown in Table 4.3, both the lower heating value and adiabatic temperature for pine wood are slightly higher compared to maple/oak wood while ammonia concentration is significantly less (maximum ammonia concentration in syngas are 199 ppm and 1060 ppm for pine and maple/oak wood respectively). Thus the lower NO_X emissions are due to lower ammonia concentration in syngas.

When comparing NO_X emissions between syngas from air blown and 40% O_2 blown gasification, pine wood shows different trends compared to maple/oak wood. The increment of NO_X emissions is highest from air blown to 30% O_2 case instead of from 30% to 40% O_2

enrichment. These trends can be seen from Figures 4.9 to 4.10—increments of 20 to 30 ppm and 10 to 15 ppm for air blown to 30% O_2 and 30% O_2 to 40% O_2, respectively. This can be explained by the ammonia concentration trends in syngas composition for pine wood. Ammonia increases from 163 ppm (for air blown) to 199 ppm and then decreases to 157 ppm (for 40% O_2 case). Nonetheless, NO_X emissions still increase monotonically from air blown, 30%, to 40% O_2. The increase in NO_X emissions from 30% to 40% O_2 case is believed due to higher thermal NO_X resulting from the higher adiabatic temperature.

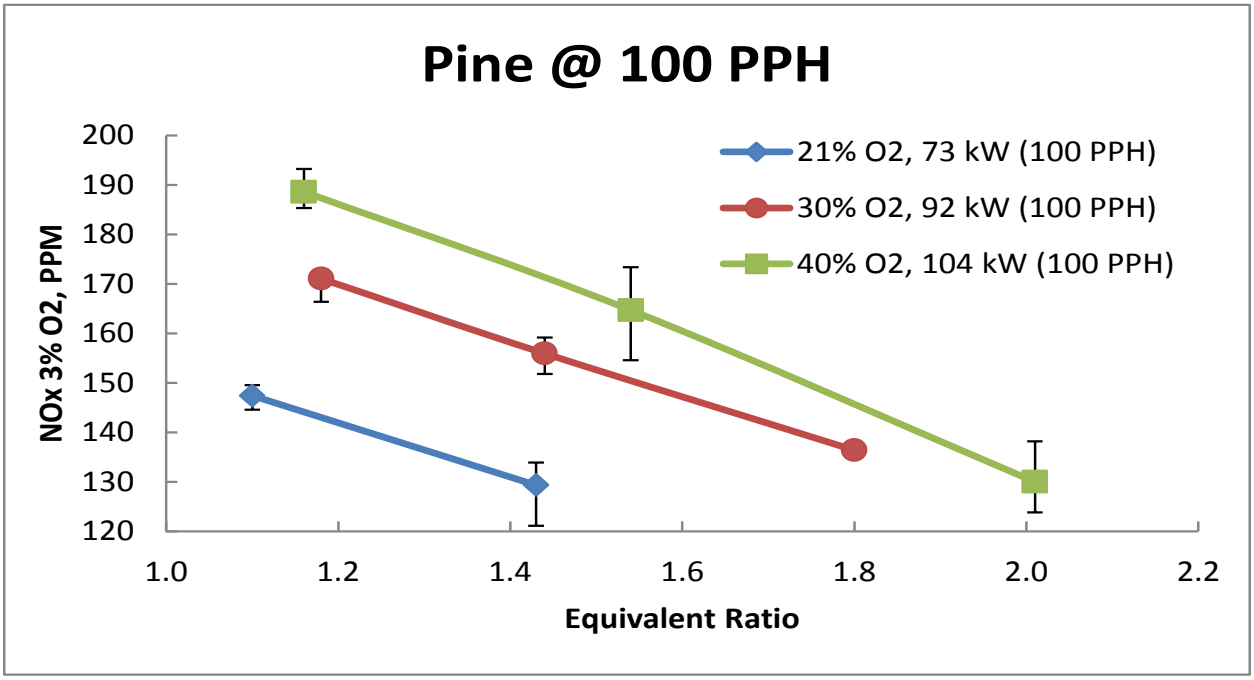

Figure 4.9: NO_x emissions comparison between air blown and oxygen enriched air-steam mixture gasification at 100 PPH.

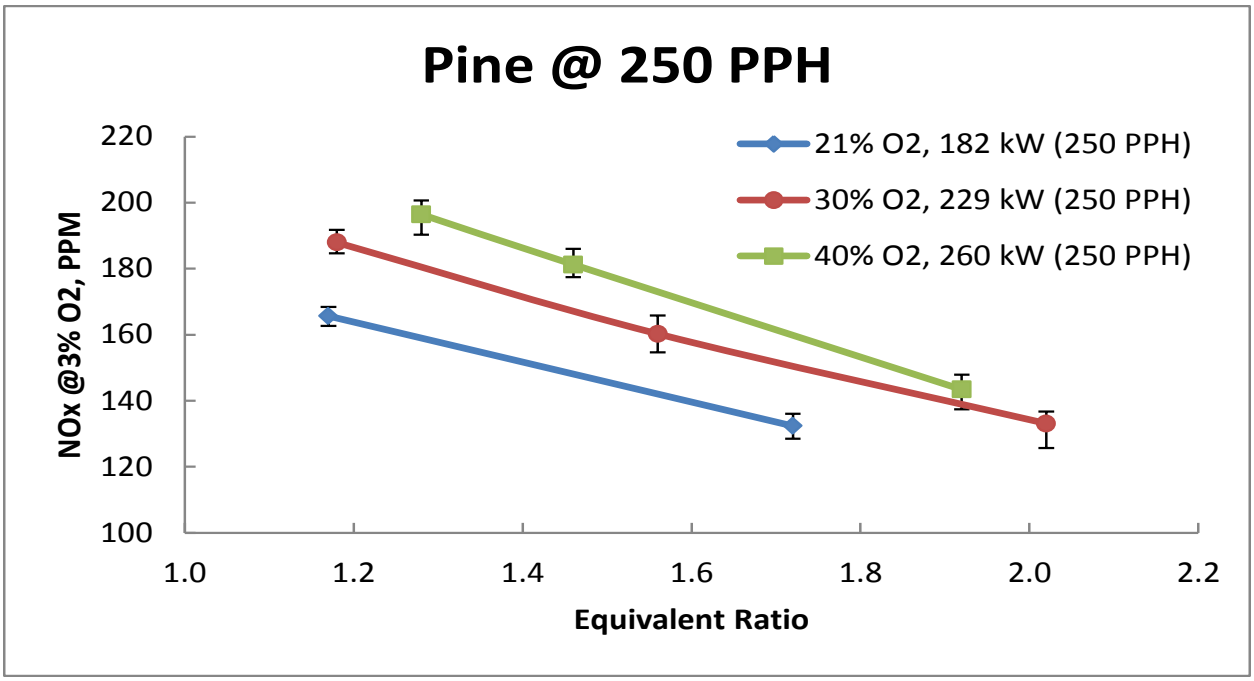

Figure 4.10: NO_x emissions comparison between air blown and oxygen enriched air-steam mixture gasification at 100 PPH.

4.4.3 –Emissions Using Seed Corn

As seen in Table 4.1, the nitrogen content for seed corn is the highest among the three feedstock studied, i.e. 1.4 wt% compared to 0.14 and 0.05 wt% for maple-oak wood and pine wood, respectively. Hence it is expected to have the highest ammonia concentration as shown in Table 4.3. The trends for NO_X emissions using seed corn at different equivalence ratios, different fueling rates, and different oxygen enriched air-steam mixture are shown in Figures 4.11 to 4.13.

Figures 4.11 to 4.13 shown that NO_X emissions from seed corn-derived syngas combustion at all gasification conditions are significantly higher compared to both maple-oak wood and pine wood at all equivalence ratios and fueling rates. The higher NO_X emissions in this case are primarily due to fuel NO_X. This can be explained as follow. The combustion temperature attained using seed corn is lower compared to pine wood and maple-oak wood due to lower its lower energy

content (lower energy content is attributed to low CO and H_2 content and high water vapor content in syngas). The adiabatic flame temperatures for each feedstock at different gasification conditions are given in Table 4.3. Therefore, thermal NO_X formed from using seed corn syngas from all gasification conditions will be lower than that of using syngas from pine wood and maple-oak wood from all gasification conditions. Additionally, according to Pershing (1976), thermal NO_X for fuel containing nitrogen species is only dominant beyond 2200 K. This temperature is well above the adiabatic flame temperatures of seed corn syngas at all gasification conditions. Furthermore, the actual flame temperature is reduced due to both heat loss to surroundings and high water content in seed corn syngas.

Opposing to the monotonic decreases in NO_X trends with leaner conditions for wood syngas, the NO_x trends for seed corn tend to reach a peak value and then decrease as conditions change from ER=1.1 to ER=2.2 (relatively lean). This trend is exhibited in all fueling rates and all oxygen enriched air conditions as shown in Figures 4.11 to 4.15. This is because at moderately lean conditions (e.g., ER=1.4 to 1.6), there is more oxygen available to oxidize ammonia to form NO_X. After all the ammonia is oxidized, the relatively leaner conditions will results in lower NO_X emissions due to lower combustion temperature. Figures 4.11 and 4.12 also show that as the fueling rate increases, the peak NO_X values tend to shift toward leaner mixtures. As the fueling rate increases, the ammonia concentration also increases. Thus, the excessive oxygen at leaner conditions is favorable for further oxidation of ammonia to NO_X.

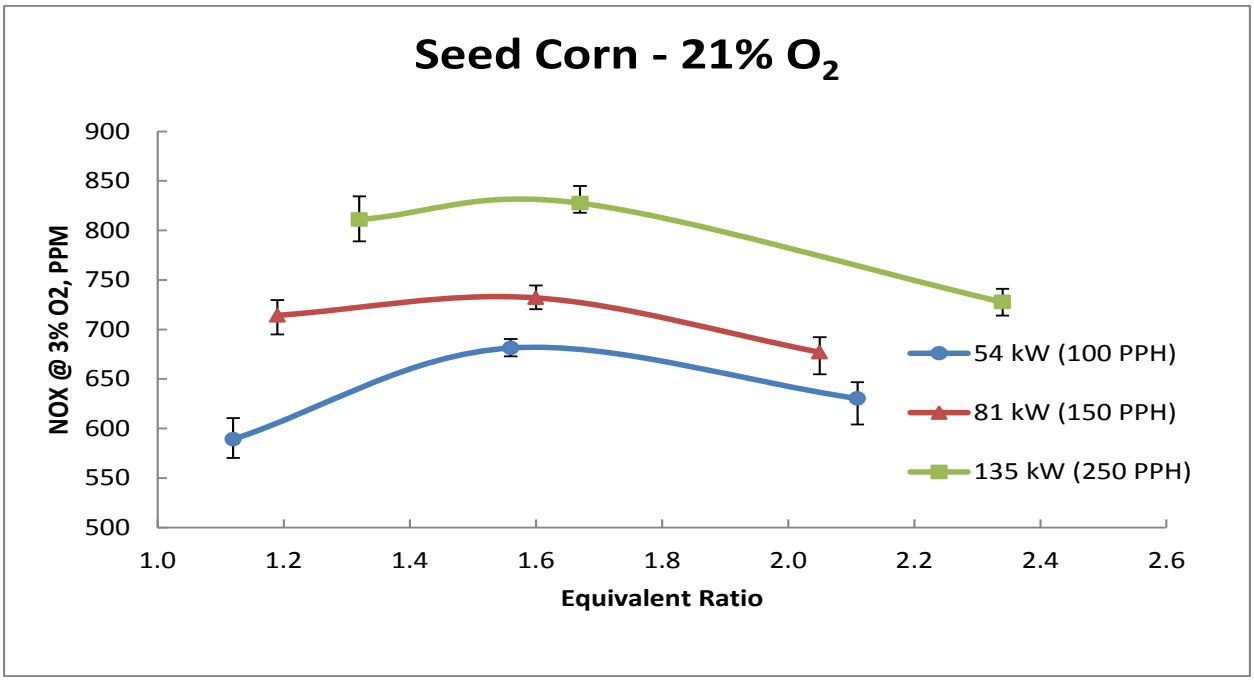

Figure 4.11: NO_X emissions using seed corn resulting from 21% air blown gasification at 100/150/250 PPH.

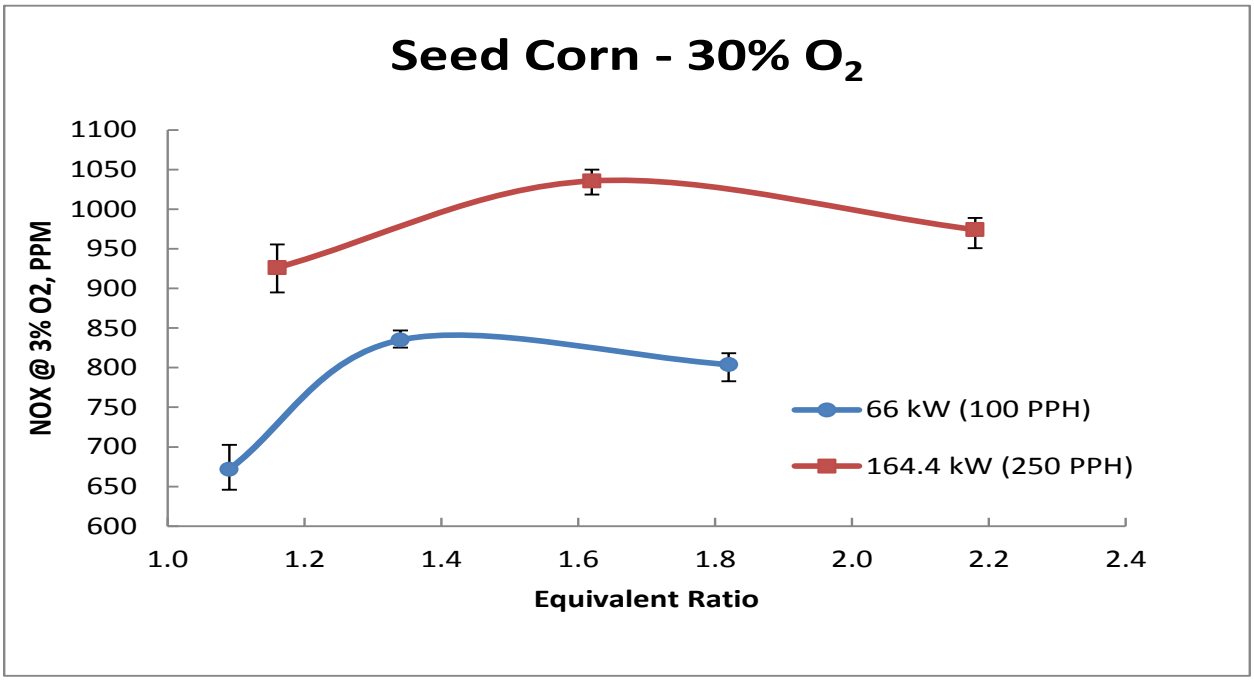

Figure 4.12: NO_X emissions using seed corn resulting from 30% oxygen enriched air-steam mixture gasification at 100/250 PPH.

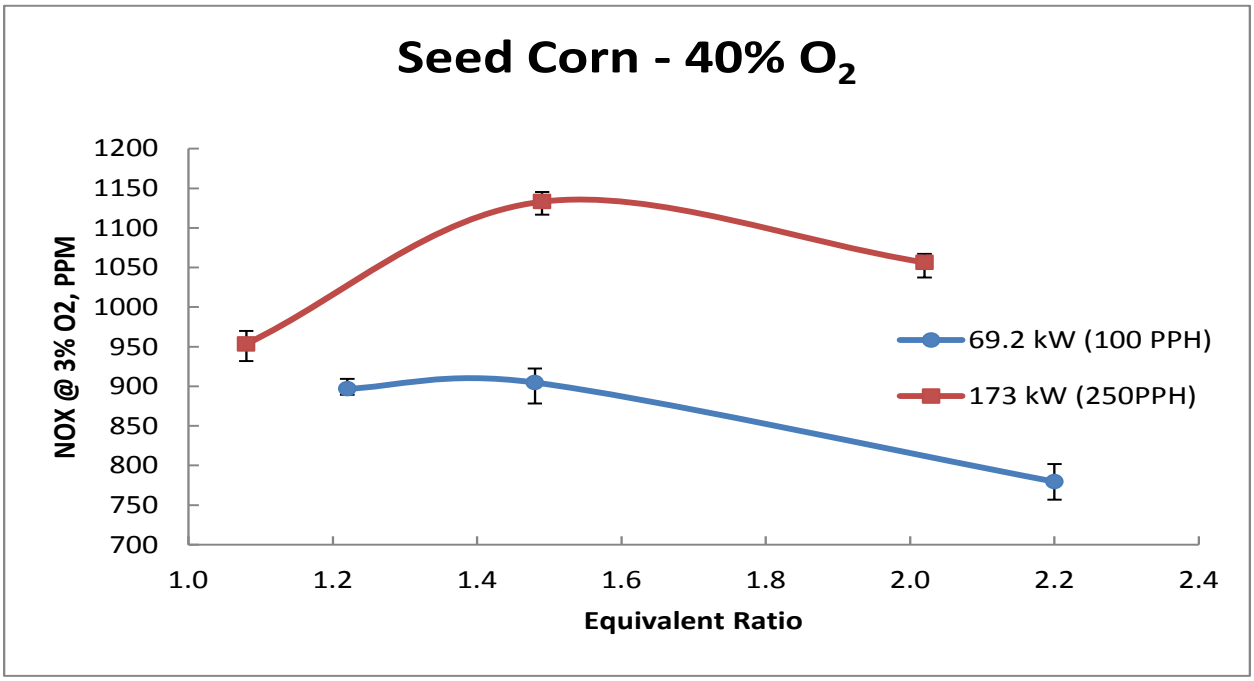

Figure 4.13: NO_X emissions using seed corn resulting from 40% oxygen enriched air-steam mixture gasification at 100/250 PPH.

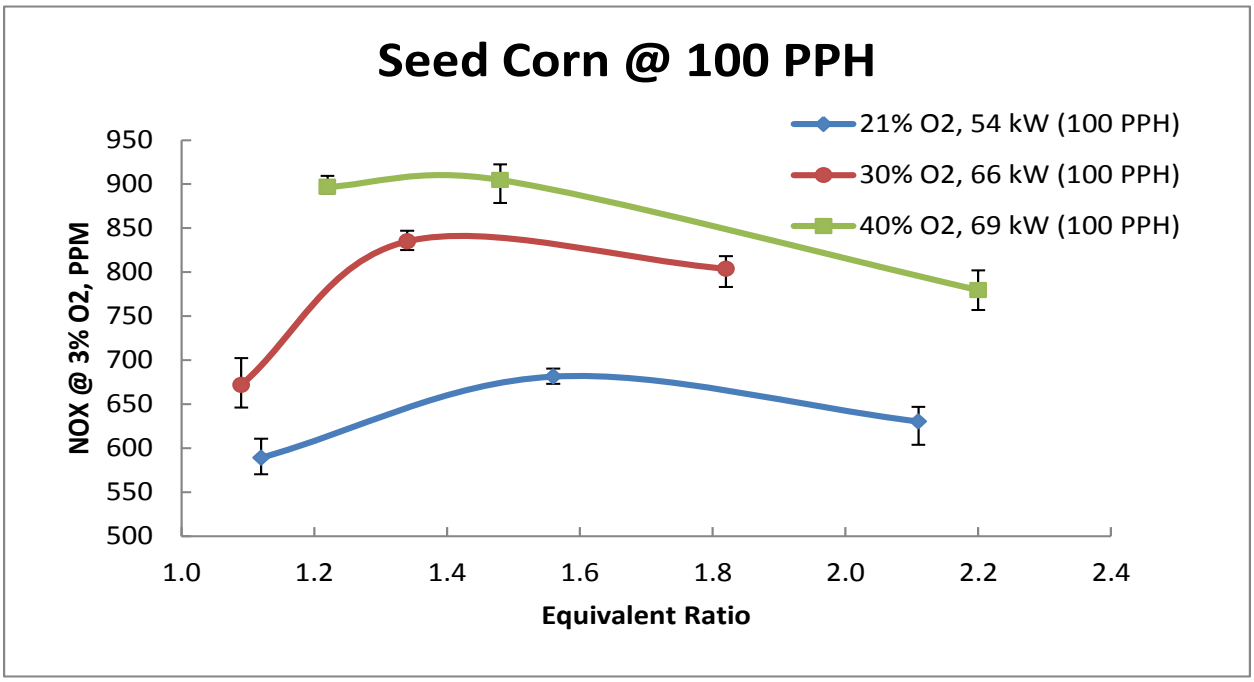

Figure 4.14: NO_X emissions comparison between air blown and oxygen enriched air-steam mixture gasification at 100 PPH.

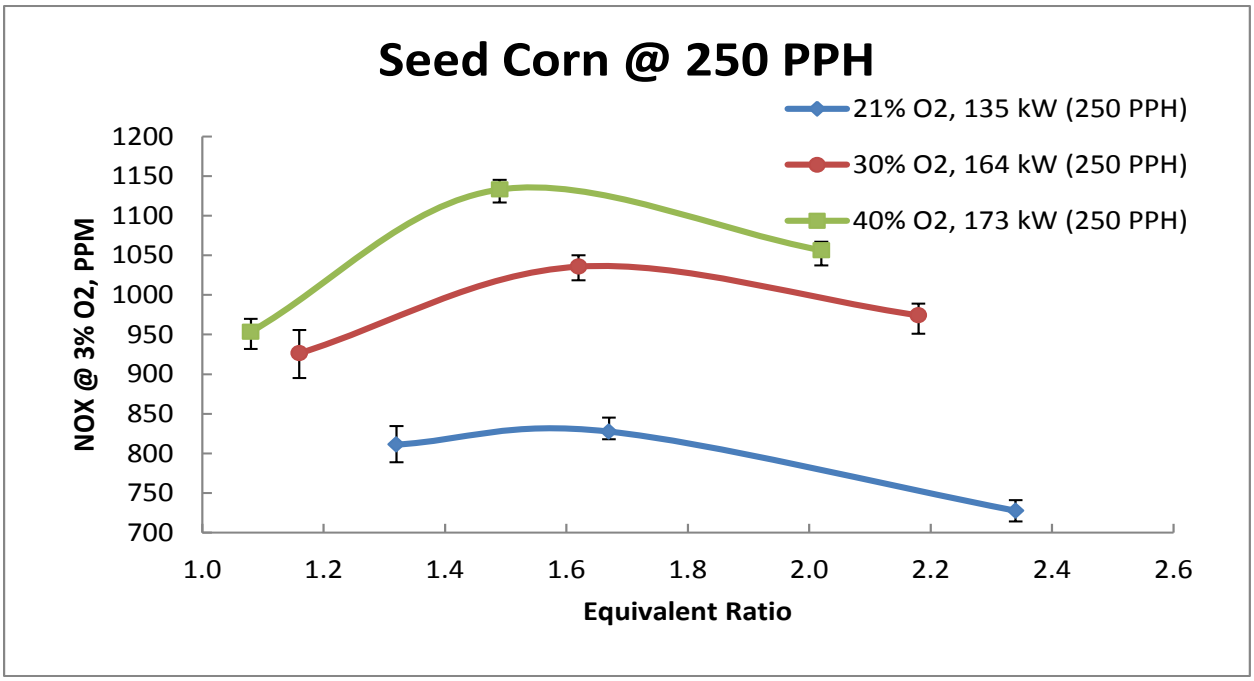

Figure 4.15: NO_X emissions comparison between air blown and oxygen enriched air-steam mixture gasification at 250 PPH.

Chapter 5 – Conclusions and Recommendations

5.1 – Conclusions

The effects of oxygen enriched air and steam mixtures on syngas compositions were studied experimentally in a pilot-scale pressurized bubbling fluidized bed reactor. In this study, the oxygen percentage in air was increased from 21% up to 40% (v/v) while keeping the steam-to-biomass ratio (S/B) and bed temperature constant at 0.17 and 800 °C, respectively. In addition, three different types of biomass feedstock of low to high nitrogen contents were selected to inspect ammonia formation in syngas at different oxygen percentages in the gasifying agent.

The use of oxygen enriched air reduces the nitrogen dilution effect, thus increasing syngas heating values. Steam contains hydrogen atoms and results in a noticeably higher production of H_2 and CH_4 in syngas across all feedstock. Moreover, breakdown of steam in a high temperature environment and through the water-gas shift reaction yields OH and H radicals. These radicals facilitate hydrogenation of active sites of char particles which contribute to significant increases in the ammonia concentration in syngas for a particular feedstock.

The study also investigated the NO_X emissions from syngas combustion using an industrial burner manufactured by ECLIPSE. The burner was specifically designed for burning natural gas and operated on the principal of non-premixed flame and staged air combustion. NO_X emissions were characterized using different operating conditions such as different fueling rates at various equivalence ratios.

For all feedstock, it was found that NO_X emissions increased as ammonia concentration in the syngas increased. Thus, NO_X emissions resulting from the fuel-NO_X pathway are very important in syngas combustion. For relatively low ammonia concentration in syngas such as when wood is used as feedstock, data showed that there was a monotonic decrease in NO_X emissions with leaner combustion and lower fuel flow rates. On the other hand, when ammonia concentration in syngas is high (i.e. syngas from seed corn), the NO_X emissions tend to reach a peak value and then decrease as conditions go leaner. Furthermore, ammonia-rich syngas exhibits shift of peak NO_X values toward leaner conditions as fueling rate increases.

5.2 – Recommendations

Although the concept of oxygen enriched-air and steam mixtures has been demonstrated as a feasible choice for gasification agent, the H_2/CO ratio is moderately low for synthesis process such as Fischer-Tropsch for conversion to liquid fuels. The required H_2/CO ratios for different liquid fuel production can be found in Table 7-8 of Higman et al., 2003. The low H_2/CO ratios are due to a large amount of unreacted steam that showed up in product gas composition. It is advisable to operate the gasifier at temperatures higher than 800 °C to promote higher water-gas shift reaction rates for more effective conversion of steam into H_2 and CH_4. Also, a more extensive test matrix needs to be developed and tested in order to find out the optimum combination of oxygen percentage in air, steam-to-biomass ratios, equivalence ratios, and bed temperatures that give the highest carbon conversion efficiency, gas LHV, and H_2/CO ratio.

In order to make syngas more viable and attractive as a renewable energy source, there is a need to explore different means of converting ammonia and other fuel-bound nitrogen species in syngas into molecular nitrogen. This would greatly help reducing the NO_X emissions from syngas combustion. Feasible options for ammonia cracking include but are not limited to: high gasification temperature and use of catalysts. Ammonia decomposes at higher temperatures where the dissociation rate depends on the pressure, the temperature, and the catalyst being used. Table A.2.2 in Appendix A.2 provides the equilibrium concentrations of ammonia as functions of the temperature for a pressure of 1 bar and 10 bars.

Finally, modification of cyclone filter is needed to achieve higher char particle capture efficiency so that full nitrogen balance can be performed. This is important for the study of how oxygen enriched-air and steam mixtures might affect the partition of biomass nitrogen in different nitrogen-containing species in syngas.

As for syngas combustion, more equivalence ratios at each fuel flow rate are recommended. The current study only covered three equivalence ratios (all at lean conditions) for each fueling rate, therefore probably did not fully capture the NO_X emission trends (especially NO_X behavior under rich conditions). Fully characterizing NO_X emission behavior will allow better understanding of syngas combustion and flame chemistry so that simulation models can be built to optimize low emissions burner design.

Appendix

A.1 – Engineering Equation Solver (EES) Code

The following code is to calculate the flame temperature of the producer gas resulting form the gasification of seed corn as the biomass feedstock at air-blown condition. The EES codes for other feedstock are similar.

```
"Tr = reactant temperature (K)
Tp = prodct temperature (K)
hr = reactant enthalpy (kJ/kmol)
hp = product enthalpy (kJ/kmol)
atom balances and first law of thermodynamics is used to find adiabatic flame temperature

mf_n2*N2+mf_co*CO+mf_h2*H2+mf_co2*CO2+mf_ch4+mf_c2h6*C2H6+mf_c2h4*C2H4+
mf_c2h2*C2H2+mf_c3h8*C3H8+mf_nh3*NH3+mf_h2o*H2O +
a(O2+3.76N2) --> d N2+b CO2+c H2O


"composition"
mf_n2     = 41.6/100
mf_co     = 12.42/100
mf_h2     = 4.43/100
mf_co2    = 10.91/100
mf_ch4    = 3.59/100
mf_c2h6 = 0.272/100
mf_c2h4 = 1.76/100
mf_c2h2 = 0.16/100
mf_c3h8 = 0.204/100
mf_nh3    = 0.53/100
mf_h2o    = 21.65/100

"check sum"
sum_molef_check =
mf_n2+mf_co+mf_h2+mf_co2+mf_ch4+mf_c2h6+mf_c2h4+mf_c2h2+mf_c3h8+mf_nh3+mf_h
2o

"atom balance"
d = a*3.76+mf_n2+mf_nh3/2
b = mf_co+mf_co2+mf_ch4+2*mf_c2h6+2*mf_c2h4+2*mf_c2h2+3*mf_c3h8
```

```
2*c = 2*mf_h2+ 4*mf_ch4+6*mf_c2h6+4*mf_c2h4+2*mf_c2h2+8*mf_c3h8+2*mf_h2o
a = b+c/2-mf_co/2-mf_co2-mf_h2o/2


"reactant properties"
Tr = 298.15
a_act = a
Pr = 1.013e5 [Pa]

"reactant enthalpy"
hrn2=ENTHALPY(N2,T=Tr)
hrco=ENTHALPY(CO,T=Tr)
hrh2 = ENTHALPY(H2,T=Tr)
hrco2=ENTHALPY(CO2,T=Tr)
hrch4=ENTHALPY(CH4,T=Tr)
hrc2h6=ENTHALPY(C2H6,T=Tr)
hrc2h4=ENTHALPY(C2H4,T=Tr)
hrc2h2=ENTHALPY(C2H2,T=Tr)
hrc3h8=ENTHALPY(C3H8,T=Tr)
hrnh3=ENTHALPY(AMMONIA,T=Tr,P=Pr)
hrh2o=ENTHALPY(H2O,T=Tr)
hro2=ENTHALPY(O2,T=Tr)

hrefco2=ENTHALPY(CO2,T=Tr)
hrefh2o=ENTHALPY(H2O,T=Tr)
hrefn2=ENTHALPY(N2,T=Tr)


"product enthalpy"
hpco2=ENTHALPY(CO2,T=Tp)
hph2o=ENTHALPY(H2O,T=Tp)
hpn2=ENTHALPY(N2,T=Tp)

"net reactant enthalpy, used for LHV"
h_reac =
(mf_n2+3.76*a)*hrn2+mf_co*hrco+mf_h2*hrh2+mf_co2*hrco2+mf_ch4*hrch4+mf_c2h6*hrc2
h6+mf_c2h4*hrc2h4+mf_c2h2*hrc2h2+mf_c3h8*hrc3h8+mf_nh3*hrnh3+mf_h2o*hrh2o+a*hr
o2

"energy balance"
h_reac = d*hpn2+b*hpco2+c*hph2o

LHV = h_reac - (d*hrefn2+b*hrefco2+c*hrefh2o)
```

A.2 - Impinger Layout, Micro G.C. Operating Conditions, and NH_3 Equilibrium Concentrations.

Figure A.2.1 shows the assembly of the stainless steel impingers where 1 is the impinger can, 2 the sanitary quick clamp, 3 the cap assembly, 4 a sintered metal filter with an 1/8 NPT fitting (further referenced to as a sparger) and 5 is a sanitary gasket.

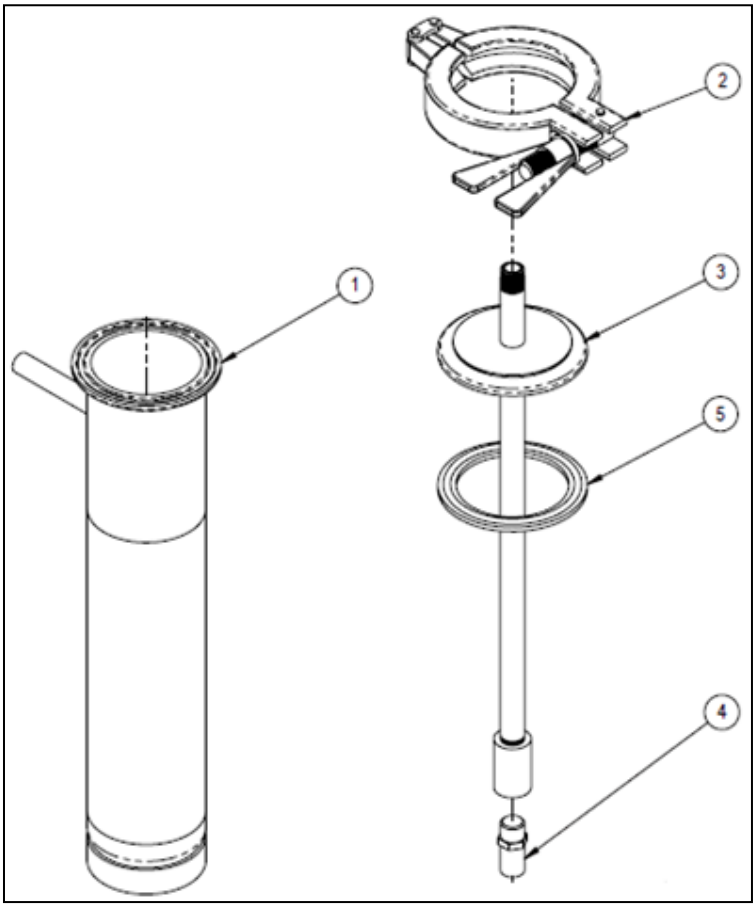

Figure A.2.1: Fabrication drawing of impinger.

Table A.2.1: Micro G.C. Operating Conditions.

Column	Measured species	Micro GC ISU	
1	He, N_2, CH_4, CO	100°C	151.6 kPa
2	C_2H_4, C_2H_2, CO_2	60°C	117.2 kPa
3	C_3H_8	60°C	55.1 kPa
4	----------	not used	not used

Table A.2.2: Equilibrium Concentration of NH_3 as Function of Temperature and Pressure (Thomas et al., 2006).

Temperature [°C]	Unconverted NH_3 at 1 bar	Unconverted NH_3 at 10 bar
400	8800ppm	7.91%
500	2600ppm	2.55%
600	1000ppm	1.00%
700	470ppm	0.47%
800	250ppm	0.25%
900	150ppm	0.15%

Bibliography

- Basu, Prabir. Biomass Gasification and Pyrolysis: Practical Design and Theory. Elsevier Inc., 2010.

- Baukal, E. Charles; Schwartz, E. Robert. The John Zink Combustion Handbook. John Zink Co., LLC 2001.

- Biomass Technology Group. Handbook: Biomass Gasification. BTG Biomass Technology Group 2005.

- Brown, Robert C. Biorenewable Resources: Engineering New Products from Agriculture. Iowa State Press 2003.

- Chen, G.; Andries, J.; Spliethoff, H.; Fang, M.; Enden, P. J. V. Biomass Gasification Integrated with Pyrolysis in a Circulating Fluidized Bed. Sol. Energy 2007, 76, 345-349.

- Campoy, Manuel; Gomez-Barea, Alberto; Vidal, B. Fernando; Ollero, Pedro. Air-Steam Gasification of Biomass in a Fluidised Bed: Process Optimisation by Enriched Air. Fuel Processing Technology 2009, 90, 677-685.

- Evans, Paul; Paskach, Thomas; Reardon, John. Detailed Kinetic Modeling to Predict Syngas Composition from Biomass Gasification in a PBFB Reactor. Wiley InterScience, 2010.

- Gil, Javier; Aznar, P. Maria; Caballero, A. Miguel; Frances, Eva; Corella, Jose. Biomass Gasification in Fluidized Bed at Pilot Scale with Steam-Oxygen Mixtures. Product Distribution for Very Different Operating Conditions. Energy & Fuels 1997, Volume 11, Number 6.

- Good, J.; Ventress, L.; Knoef, H.; Zielke, U.; Hansen, P. L.; Kamp, W. V. D. ; Wild, P. D.; Coda, B.; Passen, S. V.; Kiel, J. Sampling and Analysis of Tar Particles in Biomass Producer Gases; Technical Report; International Energy Agency, 2005.

- Higman, Christopher; Burgt, Maarten Van Der. Gasification. Elsevier Science, 2003.

- Kirkels, F. Arjan; Verbong, P. J. Geert. Biomass Gasification: Still Promising? A 30-Year Global Overview. Renewable and Sustainable Energy Reviews 2011, 15, 471-481.

- Kumar, Ajay; Eskrideg, Kent; Jones, David D.; Hanna Milford A. Steam-Air Fluidized Bed Gasification of distillers Grains: Effects of Steam to Biomass Ratio, Equivalence Ratio and Gasification Temperature. Bioresource Technology 2009, 100, 2062-2068.

- Li, C.-Z., Tan, L. L. Formation of NOx and SOx precursors during the pyrolysis of coal and biomass. Part 3. Further discussion on the formation of HCN and NH3 during pyrolysis. *Fuel*, 79, 1899-1906, 2000.

- Liu, Ke; Song, Chunshan; Subramani, Velu. Hydrogen and Syngas Production and Purification Technologies. John Wiley & Sons, Inc. 2010.

- Lv, P.M.; Xiong, Z.H., Chang; J.; Wu, C.Z., Chen, Y.; Zhu, J.X. An Experimental Study on Biomass Air-Steam Gasification in a Fluidized Bed. Bioresource Technology 2004, 95, 95-101.

- Lv, Pengmei; Yuan, Zhenhong; Ma, Longlong; Wu, Chuangzhi; Chen, Yong; Zhu, Jingxu. Hydrogen-Rich Gas Production from Biomass air and Oxygen/Steam Gasification in a Downdraft Gasifier. Renewable Energy 2007, 32, 2173-2185.

- McKenzie, Lachlan J.; Tian, Fu-Jun; Li, Chun-Zhu. NH_3 Formation and Destruction during the Gasification of Coal in Oxygen and Steam. Environ. Sci. Technol. 2007, 41, 5505-5509.

- Nakanishi, Masakazu; Ogi, Tomoko; Fukuda, Yoshio. Thermogravimetric Analysis in Steam and Oxygen with Gas Chromatograph Mass Spectrometry for Basic Study of Biomass Gasification. J Therm Anal Calorim 2010, 101, 391-396.

- Pershing DW, Wendt JOL. Pulverized coal combustion: the influence of flame temperature and coal composition on thermal and fuel NOx. Proc Combust Inst 1976; 16: 389–99.

- Pinto, Filomena; Andre, Rui Neto; Gulyurtlu, I. Innovation on Bimass Wastes Utilization Through Gasification and Co-Gasification. Stage of Deployment and Needs for Further R&D. In: Biomass Gasification: Chemistry, Processes and Applications. Nova Science Publishers, Inc., 2009.

- Ptasinski, K. J.; Jurascik, A. Sues and M. Biowastes-to-Biofuels Routes Via Gasification. In: Biomass Gasification: Chemistry, Processes and Applications. Nova Science Publishers Inc., 2009.

- Schuster, G.; Loffler G.; Weigl, K., Hofbauer, H. Biomass Steam Gasification – An Extensive Parametric Modeling Study. Bioresource Technology 2001, 77, 71-79.

- Sung, C.-J.L., Chung. Fundamental Combustion Properties of H2/CO Mixtures: Ignition and Flame Propagation at Elevated Pressures. *Combustion Science and Technology*, 2008. 180(6): p. 1097-1116.

- Thomas, George; Parks, George. Potential Role of Ammonia in Hydrogen Economy. U.S. Department of Energy, 2006.

- Tian, Fu-Jun; Yu, Jianglong; McKenzie, Lachlan J., Hayashi, Jun-ichiro; Li, Chun-Zhu. Conversion of Fuel-N into HCN and NH During the Pyrolysis and Gasification in Steam: A Comparative Study of Coal and Biomass. Energy & Fuels, 2007, 21, 517-521.

- Timmer, Kevin Jay. Carbon Conversion during Bubbling Fluidized Bed Gasification of Biomass. Iowa State University, 2008.

- Umeki, Kentaro; Yamanoto, Kouichi; Namioka Tomoaki; Yoshikawa, Kunio. High Temperature Steam-only Gasification of Woody Biomass. Applied Energy, 2010, 87, 791-798.

- U.S. Energy Information Administration. Renewable Energy Trends in Consumption and Electricity 2008. U.S. Department of Energy, 2010.

- Walter, Torres; Pansare, Sourabh S.; Goodwin Jr., James G. Hot Gas Removal of Tars, Ammonia, and Hydrogen Sulfide from Biomass Gasification Gas. Taylor & Francis Group, LLC. Catalysis Reviews, 49:407-456, 2007.

- Yu, Q-Z., Brage, C., Chen, G-X.; Sjostrom, K. The Fate of Fuel-Nitrogen during Gasification of Biomass in a Pressurised Fluidised Bed Gasifier. Fuel, 2006, 86, 611-618

- Zhou, Jiachun; Masutani, M. Stephen; Ishimura, M. Darren; Turn, Q. Scott; Kinoshita M. Charles. Release of Fuel-Bound Nitrogen during Biomass Gasification. Ind. Eng. Chem Res. 2000, 39, 626-634.

- Zhou, Jinsong; Chen, Qing; Zhao, Hui; Cao, Xiaowei; Mei Qinfeng; Luo, Zhongyang; Cen Kefa. Biomass-Oxygen Gasification in a High-Temperature Entrained-Flow Gasifier. Biotechnology Advances 2009, 27, 606-611.